DIFUNCTIONAL MONOMERIC AND POLYMERIC PHOTOINITIATORS: SYNTHESIS AND PHOTOPOLYMERIZATION BEHAVIORS

by

Belgin Cesur

B.S., Chemistry, Çanakkale Onsekiz Mart University, 2011

Submitted to the Institute for Graduate Studies in
Science and Engineering in partial fulfillment of
the requirements for the degree of
Master of Science

Graduate Program in Chemistry

Boğaziçi University

2014

DIFUNCTIONAL MONOMERIC AND POLYMERIC PHOTOINITIATORS: SYNTHESIS AND PHOTOPOLYMERIZATION BEHAVIORS

APPROVED BY:

Prof. Duygu Avcı Semiz ……..
(Thesis Supervisor)

Prof. Nergis Arsu ……

Prof. Nihan Nugay ……

DATE OF APPROVAL: 10.12.2014

Dedicated to my family…

ACKNOWLEDGEMENTS

First and foremost, I would like to deeply thank my supervisor Prof. Duygu Avcı Semiz for her systematic guidance as well as encouragement made it possible to complete this study. I gained a lot of experience thanks to her endless support and attention.

I wish to extend my deepest appreciation to my committee members Prof. Nihan Nugay and Prof. Nergis Arsu for generously giving their valuable time for reviewing the final manuscript and for their constructive comments and suggestions.

I would like to express my great thanks to Ayşe Altın Çağlayan, Özlem Karahan and Zeynep Saraylı Bilgici due to their helpfulness and guidance especially my first time in the laboratory. I also thank my dear group friends Sesil Agopcan Çınar, Tuğçe Nur Eren, Fulya Köylü, Betül Bingöl, Melek Naz Güven and Ece Akyol for their help and friendship.

I am grateful to Ayla Türkekul and Burcu Selen Çağlayan for their cooperation in NMR analysis. I would also like to thank all members of Chemistry Department who were always most helpful.

Finally, my greatest gratitude is extended to my mother, elder sister and father for their endless love, support and understanding during my whole life. My special thank is to my mother for her everlasting encouragement, love and everything…

This research was supported by The Scientific and Technological Research Council of Turkey (TÜBİTAK) [113Z241].

ABSTRACT

DIFUNCTIONAL MONOMERIC AND POLYMERIC PHOTOINITIATORS: SYNTHESIS AND PHOTOPOLYMERIZATION BEHAVIORS

The first methacrylate monomers with two Type I or Type II side-chain photoinitiating groups (PI**1**, PI**2** and PI**3**) have been synthesized from reactions of 2-(chloromethyl)acryloyl chloride and 4-hyroxybenzophenone, 4-hydroxyacetophenone or 2-hydroxy-1-[4-(2-hydroxyethoxy)phenyl]-2-methyl-1-propanone (Irgacure 2959) and polymerized to give the corresponding polymeric photoinitiators (PPI**1**, PPI**2** and PPI**3**). The photoinitiator PI**1** has also been copolymerized with N,N-dimethylaminoethyl methacrylate (DMAEM) to investigate the photoinitiation efficiency of the resulting polymer featuring built-in amine coinitiator. The photoinitiating activities of the synthesized photoinitiators together with acetophenone (AP), benzophenone (BP) and Irgacure 2959 were investigated in the photopolymerizations of hexane-1,6-diol diacrylate (HDDA) using photodifferential scanning calorimeter and the kinetic parameters have been correlated with the structures of the photoinitiating systems. The results show different photoinitiating activities compared to small molecule commercial analogs: BP-based photoinitiators, PI**1**, PPI**1** and PPI(PI**1**-*co*-DMAEM), were found to be particularly efficient compared to BP. The difunctional nature of these photoinitiators suggests the possibility (demonstrated for PI**3**) of synthesizing crosslinked copolymers even with monofunctional monomers.

ÖZET

İKİ FONKSİYONLU MONOMERİK VE POLİMERİK FOTOBAŞLATICILAR: SENTEZLERİ VE FOTOPOLİMERLEŞME DAVRANIŞLARI

Yan zincirinde iki tane I. Tip ya da II. Tip fotobaşlatıcı grupları içeren ilk metakrilat monomerleri (PI**1**, PI**2** ve PI**3**) 2-(klorometil)akriloil klorürün 4-hidroksibenzofenon, 4-hidroksiasetofenon veya 2-hidroksi-1-[4-(2-hidroksietoksi)fenil]-2-metil-1-propanon (Irgacure 2959) ile reaksiyonlarından sentezlendi ve polimerleştirilerek polimerik fotobaşlatıcılar (PPI**1**, PPI**2** ve PPI**3**) elde edildi. Fotobaşlatıcı PI**1**, N, N- dimetilaminoetil metakrilat (DMAEM) ile de kopolimerleştirilerek yapısında amin eş başlatıcısı bulunduran polimerin fotobaşlatıcı etkinliği incelendi. Sentezlenen fotobaşlatıcıların 1,6-hekzandiol diakrilat (HDDA)'ı fotobaşlatma etkinlikleri asetofenon (AP), benzofenon (BP) ve Irgacure 2959 ile birlikte foto diferansiyel taramalı kalorimetre kullanılarak incelendi ve kinetik parametreler fotobaşlatıcı sistemlerin yapılarıyla ilişkililendirildi. Sentezlenen fotobaşlatıcılar küçük molekül ticari benzerlerine göre farklı fotobaşlatma etkinlikleri gösterdi. Benzofenon içeren fotobaşlatıcıların, PI**1**, PPI**1** ve PPI(PI**1**-*co*-DMAEM), BP'a göre çok daha reaktif olduğu bulundu. Bu fotobaşlatıcılar iki fonsiyonlu yapılarından dolayı, tek fonksiyonlu monomerler ile bile çapraz bağlı kopolimerler (PI**3** için ispatlanmıştır) verebilir.

TABLE OF CONTENTS

ACKNOWLEDGEMENTS iv

ABSTRACT v

ÖZET vi

LIST OF TABLES ix

LIST OF FIGURES x

LIST OF SYMBOLS xiii

LIST OF ACRONYMS/ ABBREVIATIONS xv

1. INTRODUCTION: PHOTOPOLYMERIZATION 1

1.1. Photoinduced Free-Radical Polymerization 2

1.2. Free Radical Photoinitiators 4

1.2.1. Type I Photoinitiators 5

1.2.2. Type II Photoinitiators 7

1.3. Monomeric and Polymeric Photoinitiators 9

1.4. Monomers 22

1.5. Light sources 23

1.5.1. Xenon Lamps 24

1.5.2. Mercury Arc Lamps 24

1.5.3. Light-Emitting Diodes (LEDs) 24

1.5.4. Laser Sources 25

2. OBJECTIVES 27

3. EXPERIMENTAL WORK 28

3.1. Materials and Characterization 28

3.1.1. Materials 28

3.1.2. Characterization 28

3.2. Synthesis of Monomeric Photoinitiators 29

3.2.1. Synthesis of PI**1** 29

3.2.2. Synthesis of PI**2** 29

3.2.3. Synthesis of PI**3** 30

3.3. Synthesis of Polymeric Photoinitiators 30

3.4. Photoinitiating Activity Measurements 31

4. RESULTS AND DISCUSSIONS 32

4.1. Synthesis of Characterization of Photoinitiators 32

4.2. UV-Vis Spectral Characterization of Photoinitiators 45

4.3. Photoinitiating Activity 48

5. CONCLUSION 57

REFERENCES 58

LIST OF TABLES

Table 1.1. Structures of typical Type I photoinitiators. 6
Table 1.2. Structures of typical Type II photoinitiators. 8
Table 4.1. Solubilities of the synthesized photoinitiators in selected solvents. 32
Table 4.2. Synthesis and characterization data for polymeric photoinitiators. 43
Table 4.3. Absorption properties of the synthesized phtoinitiators compared with AP, BP and Irgacure 2959 in chloroform solution. 46

LIST OF FIGURES

Figure 1.1. Photopolymerization process [6]. 1
Figure 1.2. Reaction steps in a photoinitiated free-radical polymerization. 2
Figure 1.3. Primary processes occuring in the excited state of a UV radical initiator. .. 5
Figure 1.4. Homolytic cleavage reaction of a Type I photoinitiator. 5
Figure 1.5. Photofragmentation process for a DMPA [13]. 7
Figure 1.6. Formation of radicals from photolysis of Type II photoinitiator. 7
Figure 1.7. Structures of some amine synergists. 9
Figure 1.8. Photofragmentation process for PPIs containing benzoin methyl ether moieties [15]. 11
Figure 1.9. Examples of phosphine oxide photoinitiating monomers [16]. 12
Figure 1.10. Structures of monomeric photoinitiators containing Irgacure 2959 or BP moieties [17]. 12
Figure 1.11. The mechanism of polymerization initiated by polysiloxane-modified photoinitiators [18]. 13
Figure 1.12. Polymeric TX photoinitiators synthesized by click reaction [6]. 13
Figure 1.13. PPIs containing in-chain BP and amine [20]. 14
Figure 1.14. The structure of PEG-BP photoinitiator [22]. 15
Figure 1.15. Structure of a sulfur-containing PPI with side-chain BP groups [23]. 15
Figure 1.16. BP-containing RHMA based photoinitiators [26]. 16
Figure 1.17. Synthesis of TX-containing PPIs [27]. 16
Figure 1.18. Structure of a photoinimer [29]. 17
Figure 1.19. The representation of the intramolecular excitation energy transfer from the TX triplet state to the ground state α-morpholino-acetophenone chromophore [30]. 18
Figure 1.20. Examples of PPIs of Type II [4]. 18
Figure 1.21. Structure of a camphorquinone-based PPI [32]. 19
Figure 1.22. Synthesis of multifunctional hyperbranched PPIs [34]. 20
Figure 1.23. Synthesis of a photoinitiator containing BP with built-in tertiary amine from trimethylolpropanetriacrylate [37]. 21

Figure 1.24. Synthesis of hyperbranched PPI with built-in aliphatic tertiary amine coinitiator [38]. 21
Figure 1.25. Synthesis of a hyperbranced PPI from poly(ethylene imine) [40]. 22
Figure 1.26. Wavelength output comparison of mercury-arc and UV-LED lamps. 25
Figure 4.1. Synthesis of photoinitiators bearing two side-chain photoinitiating moieties. 33
Figure 4.2. ^{1}H NMR spectra of PI**1** and PPI(PI**1**-*co*-DMAEM). 35
Figure 4.3. ^{1}H NMR spectra of PI**2** and PPI**2**. 36
Figure 4.4. ^{1}H NMR spectrum of PI**3**. 37
Figure 4.5. ^{13}C NMR spectrum of PI**1**. 38
Figure 4.6. ^{13}C NMR spectrum of PI**3**. 39
Figure 4.7. FTIR spectra of PI**1** and PPI**1**. 40
Figure 4.8. FTIR spectra of PI**2** and PPI**2**. 41
Figure 4.9. FTIR spectra of PI**3** and PPI**3**. 42
Figure 4.10. T_g analysis of polymeric photoinitiators. 44
Figure 4.11. TGA traces of PPI(PI**1**-*co*-DMAEM) (20:80 mol %), PPI(PI**1**-*co*-DMAEM) (13:87 mol%), PPI**1**, PPI**2**, PPI**3**. 45
Figure 4.12. UV-Vis absorption spectra of AP, BP, Irgacure 2959, PI**1**, PI**2** and PI**3** in chloroform ($4x10^{-5}$ M) solution. 47
Figure 4.13. UV-Vis absorption spectra of PPI**1**, PPI**2**, PPI**3** and PPI**(**PI**1**-*co*-DMAEM) in chloroform ($4x10^{-5}$ M) solution. 47
Figure 4.14. Rate-time and conversion-time plots for the photopolymerization of HDDA initiated by BP/DMAEM, PI**1**/poly-DMAEM, AP/DMAEM, PI**2**/DMAEM, PI**1**/DMAEM. Photoinitiator and amine concentration in monomer are 1 and 3 mol%. 49
Figure 4.15. Rate-time and conversion-time plots for the photopolymerization of HDDA initiated by PI**1**(0.5 mol %)/DMAEM(1.5 mol %), PI**1**(0.5 mol %)/DMAEM(3 mol %),PI**1**(1 mol %)/DMAEM(3 mol %). 50
Figure 4.16. Rate-time and conversion-time plots for the photopolymerization of HDDA initiated by PPI**1**/poly-DMAEM, PPI**2**/DMAEM, PPI**1**/DMAEM. Photoinitiator and amine concentration in monomer are 1 and 3 mol%. ... 51

Figure 4.17. Rate-time and conversion-time plots for the photopolymerization of HDDA initiated by PPI(PI**1**-*co*-DMAEM) (13:87 mol %), PPI(PI**1**-*co*-DMAEM) (20:80 mol %), PI**1**/DMAEM (12:88 mol %). 52

Figure 4.18. Rate-time and conversion-time plots for the photopolymerization of HDDA initiated by Irgacure 2959, PPI**3**, PI**3**. Photoinitiator concentration in monomer is 2 mol%. 53

Figure 4.19. Rate-time and conversion-time plots for the photopolymerization of PI**3**. 54

Figure 4.20. Photoinitiated free radical polymerization of butyl methacrylate by using PI**3**. 56

LIST OF SYMBOLS

[I]	Concentration of the initiator
k_{diss}	The dissociation rate constant
k_p	The rate constant of the propagation reaction
k_t	The rate constant of the termination reaction
M	The molar mass of the monomer
M_n	The number average molecular weight
N	The number of double bonds per monomer molecule
PI	Photoinitiator
PPI	Polymeric photoinitiator
PI**1**	4-benzoylphenyl-2-((4-benzoylphenoxy)methyl)acrylate
PI**2**	4-acetylphenyl-2-((4-acetylphenoxy)methyl)acrylate
PI**3**	2-(4-(2-hydroxy-2-methylpropanoyl)phenoxy)ethyl-2-((2-(4-(2-hydroxy-2-methylpropanoyl)phenoxy)ethoxy)methyl)acrylate
Q/ s	Heat flow per second
R_i	Rate of initiation
R_{pmax}	The maximum rate of polymerization
R_p	Rate of polymerization
ΔH_p	Heat released per mole of double bonds reacted
ε	Extinction coefficient
I_a	Intensity of absorbed light
λ_{max}	The wavelengths for maximum absorption

Φ	Number of propagation chains initiated per light photon absorbed

LIST OF ACRONYMS/ ABBREVIATIONS

AIBN	2,2'-Azobisisobutyronitrile
AP	Acetophenone
BP	Benzophenone
CMAC	2-(Chloromethyl)acryloyl chloride
CQ	Camphorquinone
DABCO	1,4-Diazabicyclo[2.2.2]octane
DMAEM	N,N-dimethylaminoethyl methacrylate
DMPA	2,2-Dimethoxy-2-phenylacetophenone
DSC	Differential Scanning Calorimetry
FT-IR	Fourier Transform Infrared Spectroscopy
GPC	Gel Permeation Chromatography
HDDA	Hexane-1,6-diol diacrylate
IRGACURE 2959	2-Hydroxy-1-[4-(2-hydroxyethoxy)phenyl]-2-methyl-1-propanone
NMR	Nuclear Magnetic Resonance spectroscopy
RHMA	Alkyl α--hydroxymethacrylate
TBBr	*Tert*-butyl α–bromomethacrylate
TBHMA	*Tert*-butyl α–hydroxymethacrylate
TEA	Triethylamine
TEGDMA	Triethyleneglycol dimethacrylate
T_g	Glass transition temperature

TGA	Thermal Gravimetric Analysis
THF	Tetrahydrofuran
TX	Thioxanthone

1. INTRODUCTION: PHOTOPOLYMERIZATION

Photopolymerization science and technology is a field of great significance due to its environmental and manufacturing advantages [1-2]. Photopolymerization processes have many advantages compared to the thermal polymerization processes, such as reduced VOC emissions [3] due to solvent-free formulations, lower energy requirements and shorter curing times due to high rate of polymerization at ambient temperature, leading to a more efficient manufacturing process. Furthermore, they also provide spatial and temporal control of the polymerization. Due to these advantages, photopolymerization technology has been used for various applications including coatings, inks, adhesives, printings, dental fillings, photolithography and electronics [4-8].

Photopolymerization formulations are composed of monomers or oligomers and a small amount of a photoinitiator. Light causes the generation of active centers or reactive species from the photoinitiator. Active centers which may be either free radicals or cations react with monomers and oligomers and cause polymerization and/or crosslink (Figure 1.1). Regarding to the active centers, photoinitiated polymerizations can be cationic and free radical polymerizations [9].

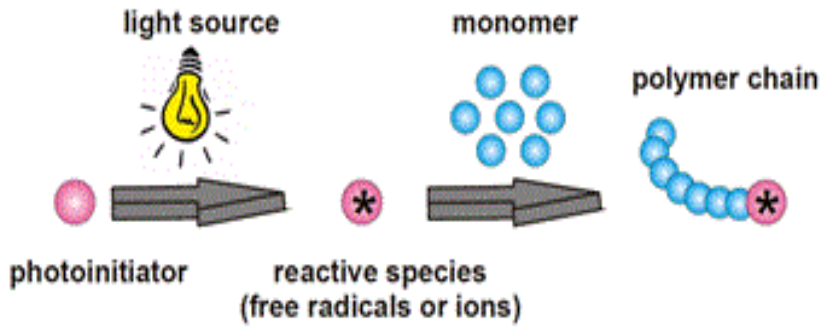

Figure 1.1. Photopolymerization process [6].

1.1. Photoinduced Free-Radical Polymerization

Photoinitiated free radical polymerization is widely used in industrial applications due to its applicability to a wide range of monomers and oligomers such as (meth)acrylates, (meth)acrylamides, unsaturated esters, etc. A typical free-radical polymerization consists of four steps (Figure 1.2): photoinitiation, propagation, chain transfer and termination [9].

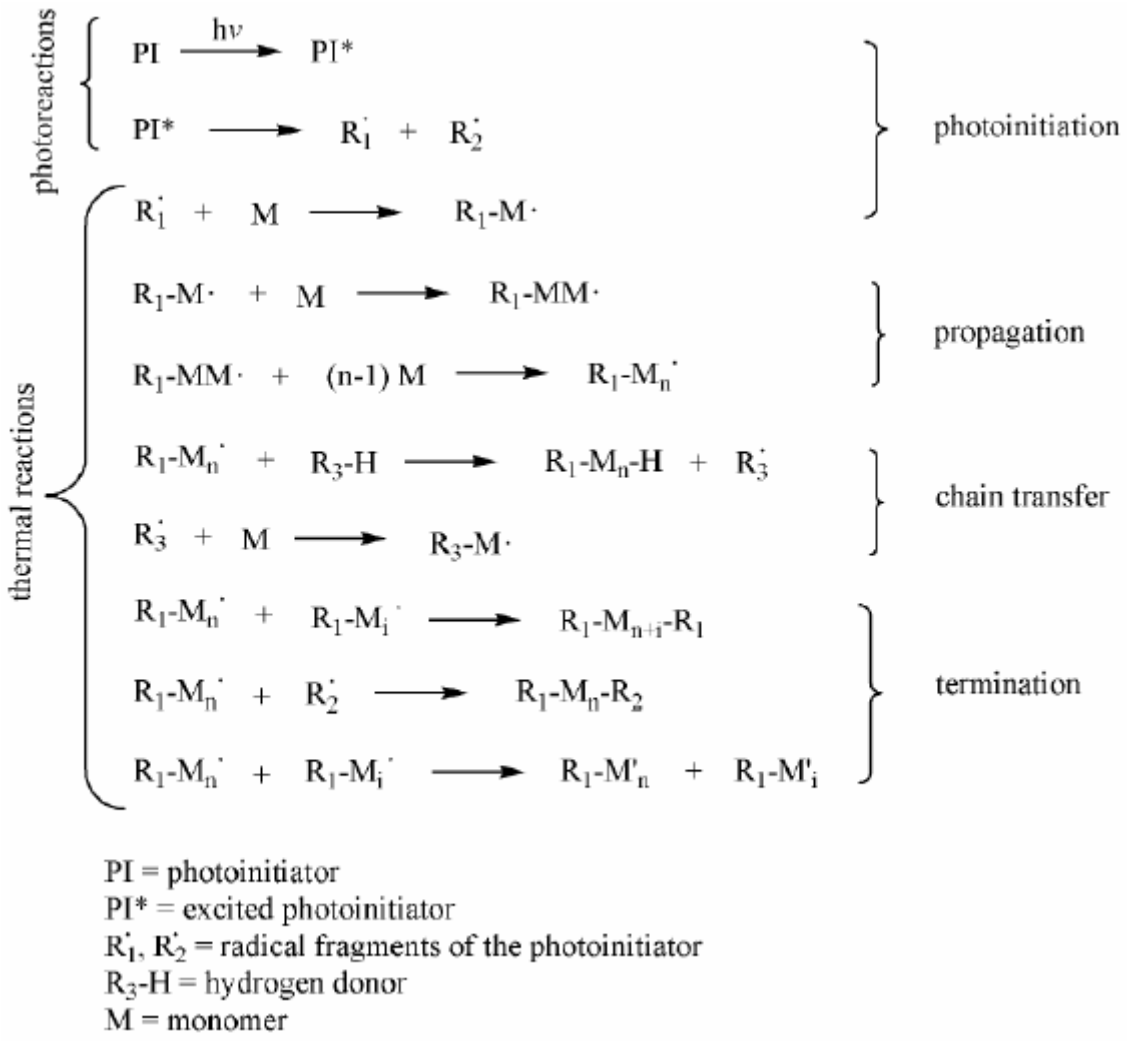

Figure 1.2. Reaction steps in a photoinitiated free-radical polymerization.

The first step, photoinitiation, involves absorption of light by a photosensitive compound or transfer of electronic excitation energy from a sensitizer to the photosensitive compound. Homolytic bond cleavage leads to the formation of a radical that reacts with monomer [10]. The propagation step involves the addition of monomer units to the chain radical to produce the polymer backbone. The chain transfer step includes termination of growing chains by hydrogen abstraction from various species (e.g, from solvent, the remaining unreacted monomer) and production of new radical capable of initiating another chain reaction [10]. The termination reactions consume radicals without generating other radicals.

The rate of initiation (R_i) shows the rate of generation of PI* and is given by

$$R_i = 2\Phi I_a \tag{1.1}$$

The term Φ represents the initiation quantum yield that is, the number of propagation chains initiated per photon absorbed. I_a is the intensity of absorbed light (called einstein in photochemistry) in moles of light quanta per liter-second. The factor of 2 represents that two radicals are generated per molecule undergoing photolysis, and is not used for those initiating systems that yield only one radical. The maximum value of Φ is 1 for all photoinitiating systems. R_i can also be written as

$$R_i = 2\Phi\varepsilon I[\mathrm{PI}]h \tag{1.2}$$

where I is the incident light intensity, Φ is the quantum yield of formation of radicals, ε is the molar extinction coefficient of the photoinitiator and h the thickness of the irradiated sample.

The rate of the polymerization R_p is given by

$$R_p = k_p[M](R_i/2k_t)^{1/2} \tag{1.3}$$

Where [M] is the monomer concentration, R_i is the rate of initiation, k_p is the propagation rate constant and k_t is the termination rate constant.
Combining Equations 1.1 and 1.3 we get

$$R_p = k_p[M](\Phi\varepsilon[I]h/k_t\ )^{1/2} \qquad (1.4)$$

1.2. Free Radical Photoinitiators

The absorption of incident light by both monomeric and polymeric formulations generally does not lead to generation of free radicals. Indeed, no polymerization reactions can occur unless a photoinitiator system is used. A photoinitiator or photoinitiator system is a compound or combinations of molecules which, when exposed to irradiation, can induce polymerization at a much faster rate than would occur in their absence.

The role of photoinitiator is to absorb the light effectively and generate reactive species that will initiate polymerization. When a photon is absorbed by the photoinitiator molecule, the energy is used to promote an electron from a bonding or non-bonding molecular orbital to an antibonding orbital. For most commonly used initiators and photosensitizers bonding molecular orbitals are usually π orbitals and non-bonding orbitals are n-orbitals. The typical C = O chromophoric group has both π and n-bonding orbitals and promotion of electron will occur from these orbitals to π^* orbital. When the photon absorption is very fast spin will be conserved and excited singlet states (S_1, S_2, ...S_n) will be generated (Figure 1.3). The excited molecule can either go back to the ground state by emitting energy (fluorescence) or it can pass to the excited triplet state. The relaxation to the ground state has relatively short lifetimes (about 10^{-9}- 10^{-6} s). A change in the spin state of the electronically excited molecule will produce triplet states (T_1, T_2....T_n) with two unpaired spins. This process is called intersystem crossing (ICS) and it is a slow process (about 10^{-11}-10^{-6} s) compared to the absorption. Triplet states are always lower in energy than the corresponding singlet states. Molecules in the triplet state generate free radicals which initiates polymerization and/or crosslinking reactions or they can return to the ground state by spin inversion (phosphorescence). Since spin inversion is a slow process the triplet states often have long lifetime (10^{-8}-10^{-3} s).

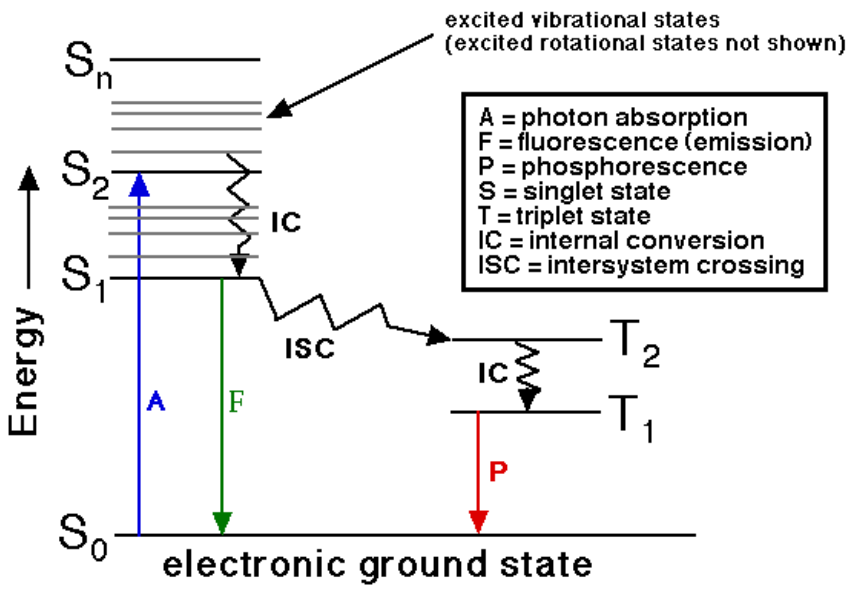

Figure 1.3. Primary processes occuring in the excited state of a UV radical initiator.

Photoinitiators take a pivotal role by managing both the rate of initiation and the penetration of incident light into the sample, and therefore control the depth of cure. It is possible to achieve a deep-through cure by preferring a photonitiator (PI) having the highest initiation efficiency and undergoing fast photobleaching upon UV exposure.

Radical generation from photoinitiator molecules can occur via two possible reaction processes that are designated as Type I and Type II reactions.

1.2.1. Type I Photoinitiators

A Type I photoinitiator is cleaved homolytically by absorbing photons, which is called α–cleavage, and generates free radicals capable of inducing polymerization (Figure 1.4).

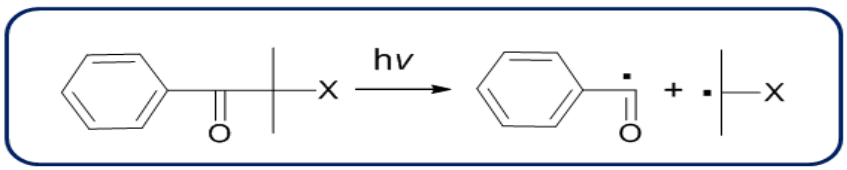

Figure 1.4. Homolytic cleavage reaction of a Type I photoinitiator.

Aromatic carbonyl compounds containing proper substituent are able to directly fragment, thereby producing radicals, form the majority of Type I photoinitiators (PIs) (Table 1.1). The benzoyl radical is the major initiating radical, while the other may also contribute to the initiation. A significant criterion for a Type I photoinitiator is the existence of a bond with a dissociation energy lower than the excitation energy of the reactive excited state, but adequately high to provide sufficient thermal stability [12]. Type I photoinitiators are not quenched by oxygen due to their short excited state lifetimes. This property makes them convenient for curing applications in the air. On the other hand, Type I compounds lead to volatile photodecomposition products because of the cleavage mechanism and add to the migration and odour problems. Figure 1.5 shows the fragmentation of one of the most commonly used Type I photoinitiators, DMPA (2,2-dimethoxy-2-phenylacetophenone) [13].

Table 1.1. Structures of typical Type I photoinitiators.

Photoinitiators	**Structure**	**λ_{max} (nm)**
Benzoin ethers	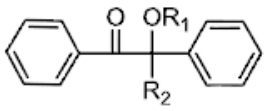 R_1=H, alkyl R_2=H, substitued alkyl	323
Benzil ketals	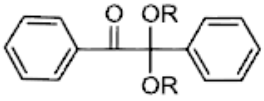 R=CH_3, C_3H_7,CH_2	365
Acylphospine oxides	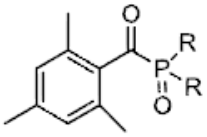 R=C_6H_5, OCH_3	380
Aminoalkyl phenones	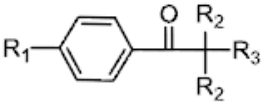 R_1=SCH_3, morpholine R_2=CH_3, CH_2P, C_2H_5 R_3=$N(CH_3)_3$, morpholine	320

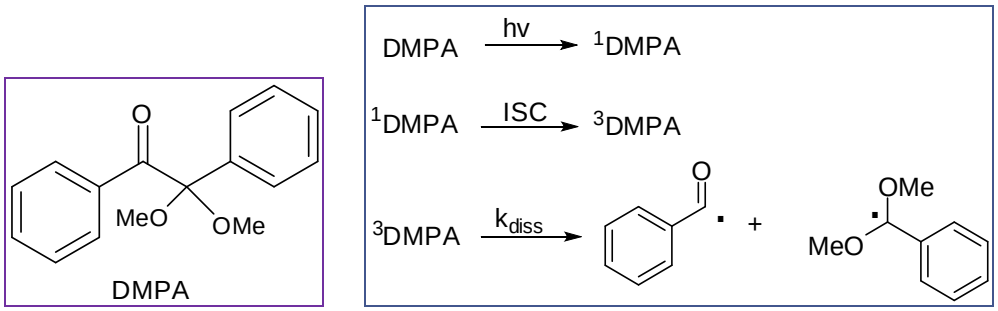

Figure 1.5. Photofragmentation process for a DMPA [13].

1.2.2. Type II Photoinitiators

A Type II photoinitiator is composed of a photosensitizer and a coinitiator that undergo a bimolecular reaction where the excited state of the photosensitizer interacts with the coinitiator to generate free radicals. The overall mechanism of the photoinitiation on the example of benzophenone (BP) is presented in Figure 1.6. Upon irradiation, a ketyl radical from the carbonyl compound and alkyl radical from the hydrogen donor are produced. The ketyl radical formed from BP is not reactive toward double bonds because of steric hindrance and delocalization of the unpaired electron. Moreover, ketyl radicals are known as terminating agents of the growing polymer chain or give side products. Therefore, the initiation occurs from the radical of the hydrogen donor [6].

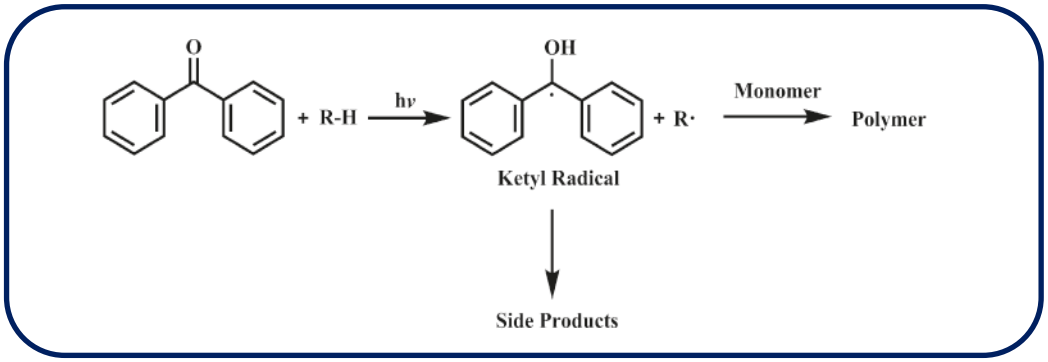

Figure 1.6. Formation of radicals from photolysis of Type II photoinitiator.

A large number of aromatic ketones (BP, substituted BPs, benzils, fluorenone, xanthone and thioxantones) will act as Type II initiators and their performance is enhanced

by tertiary amine synergists (Table 1.2 and Figure 1.7). Tertiary amines are more reactive co-initiators than alcohols or ethers. Thiols are another class of co-initiators in thiol-ene polymerization systems [6]. Recently, the studies have showed that it is possible to synthesize Type II photoinitiators without using an additional H-donor compound [14].

Table 1.2. Structures of typical Type II photoinitiators.

Photoinitiators	Structure	λ_{max} (nm)
Benzophenone	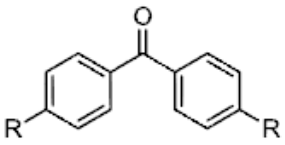 R=H, OH, $N(C_2H_5)_2$, C_6H_5	335
Thioxanthones	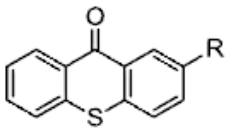 R=H, Cl, isopropyl	390
Coumarins	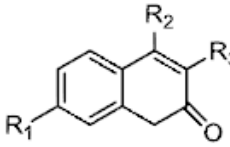 R_1=$N(C_2H_5)_2$, $N(CH_3)_2$ R_2=CH_3, eyelopentane R_3=benzothiazole, H	370
Benzils	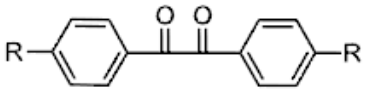 R=H, CH_3	340

There are essentially two classes of amine synergists, aliphatic and aromatic, with different characteristics and uses (Figure 1.7). Aliphatic amines are transparent down to about 260 nm and, ultimately, a coating containing such amines can be cured with UV light down to that wavelength. Aromatic amine synergists exhibit strong absorption around 300 nm and, hereby screen much of the UV light. Therefore, in cures with BP it is best to use an aliphatic amine, whereas thioxanthones, because of their strong absorption at wavelengths greater than 400 nm, can be used successfully with an aromatic amine.

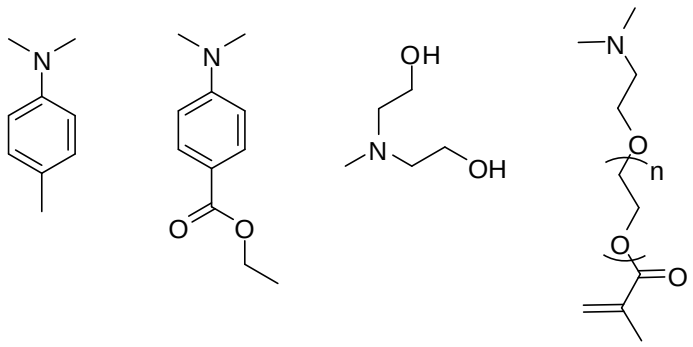

Figure 1.7. Structures of some amine synergists.

Since the initiation in Type II photoinitiator systems depends on bimolecular reactions as mentioned above, generation of radicals from Type II photoinitiators and their curing rates are generally slower than the unimolecular generation of free radicals from Type I photoinitiators. Type II photoinitiators in combination with alcohols or ethers are susceptible to oxygen quenching, because of the relatively long lived triplet states of these ketones. If amines are used as coinitiators, the primary radicals are mainly formed in an exciplex. Exciplex formation is not affected by oxygen and, as for Type I photoinitiators, radical scavenging is responsible for the observed oxygen inhibition. Whilst Type I compounds give rise to volatile photodecomposition products, the Type II photoinitiators have a more favorable profile because the ketyl radical either is re-oxidized back to the ketone or leads to recombination products with formation of higher molecular weight derivatives with a lower volatility than parent compounds.

1.3. Monomeric and Polymeric Photoinitiators

During photopolymerization, unreacted photoinitiator molecules and/or less reactive photoinitiator fragments may migrate out of the materials. Because these compounds are toxic, migration is undesirable, especially for biomedical applications. Also, low solubility of the photoinitiators in acrylate formulations is another problem. Moreover, an increase of the photoinitiation activity is desirable in terms of reduction of exposure time and increase of productivity. Hence, the development of novel photoinitiators endowed with better properties such as high photoreactivity, good solubility in the formulation, low odor and toxicity, no darkening due to the migration of residues in the cured film and good

storage stability has become an important issue [4]. Therefore in recent years, polymerizable, oligomeric or polymeric photoinitiators (PPIs) meeting most of the above mentioned requirements received continued interest due to their advantages in comparison with their corresponding low molecular weight non-monomeric analogues.

PPIs are macromolecules containing side or main chain photosensitive groups which generate free radicals by direct fragmentation, hydrogen abstraction or electron transfer upon absorption of light to initiate polymerization. A variety of PPIs containing Type I (e.g. benzoin derivatives, benzil ketals, acetophenone derivatives) and Type II (e.g. BP, TX, anthraquinone, camphorquinone or benzyl moieties) free radical photoinitiators were designed to improve photoinitiating activities in the literature.

Benzoin ether derivatives have been preferred as efficient UV radical photoinitiators for a long time. They were applied to various UV polymerizable systems such as surface protecting coatings, photoresists and adhesives. Polymers having benzoin methyl ether moieties linked to the main chain through the α-methylol group and the benzoin group linked to the carboxy group through the para position of the benzyl ring have been examined [15] (Figure 1.8). These systems display very different photoinitiating activities. Upon irradiation the former gives a free benzoyl radical and the polymer-bound α-alkoxybenzyl radical. However, the other polymer gives polymer-bound benzoyl radical and a low molecular weight α-alkoxybenzyl radical. Benzoyl radicals are more active as initiating species than α-alkoxybenzyl radicals which are involved mainly in the termination reactions. The higher reactivity of the first polymer can be explained by the reduced termination reaction by the polymer-bound α-alkoxybenzyl radical, due to the steric hindrance by polymer coiling [15].

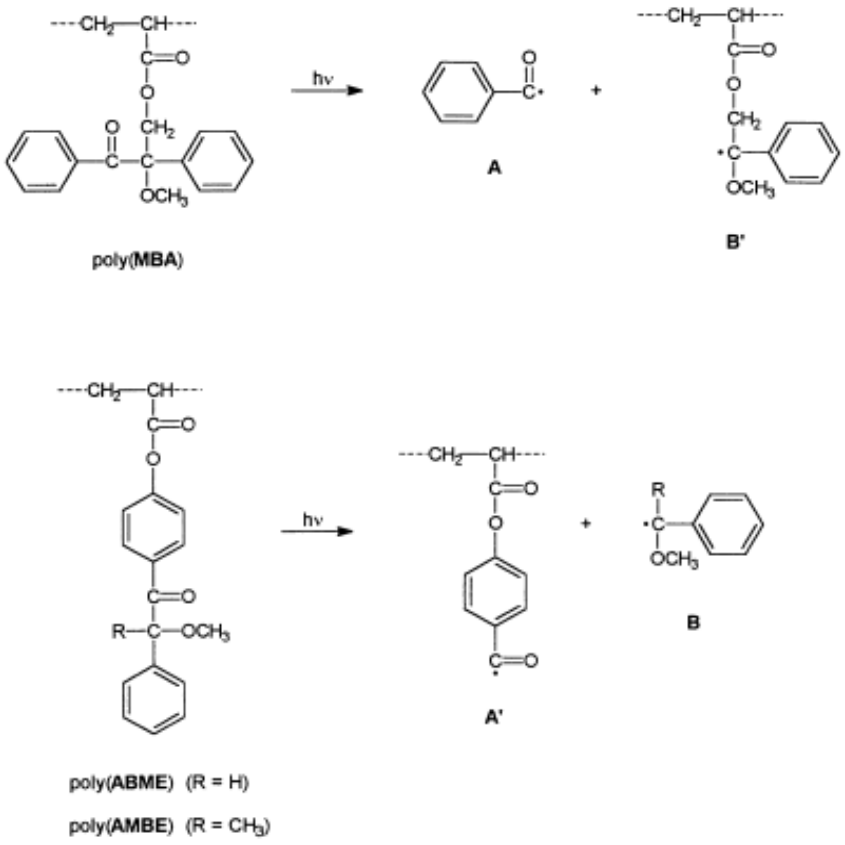

Figure 1.8. Photofragmentation process for PPIs containing benzoin methyl ether moieties [15].

Vinyl-functionalized phosphine oxide photoinitiating monomers which can be used for wavelengths up to 420 nm have been synthesized and copolymerized with vinyl acetate, vinylpyrrolidone and dimethylacrylamide (Figure 1.9). The polymeric photoinitiator releasing a phosphinoyl oxide radical is expected to be more efficient than carbonyl radical releasing polymeric photoinitiators. Also, radicals in the polymer backbone have a reduced reactivity because of their reduced mobility. Therefore, the difference between the two PPIs are comparable to the difference between the carbonyl and phosphinoyl radicals and the radical retained in the polymer backbone also initiates the reaction. Therefore, the polymer is incorporated into the polymer network serving as a crosslinker which is an advantage above low-molecular weight photoinitiators [16].

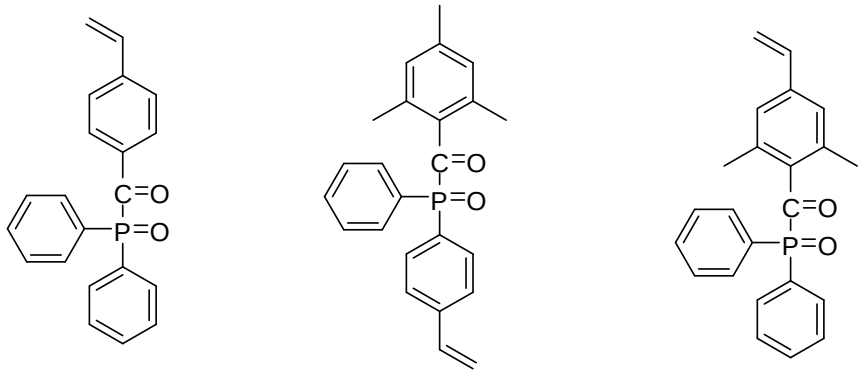

Figure 1.9. Examples of phosphine oxide photoinitiating monomers [16].

Both acrylation and binding of Irgacure 2959 to the melamine acrylate resin was found to display low photoactivity (Figure 1.10) [17].

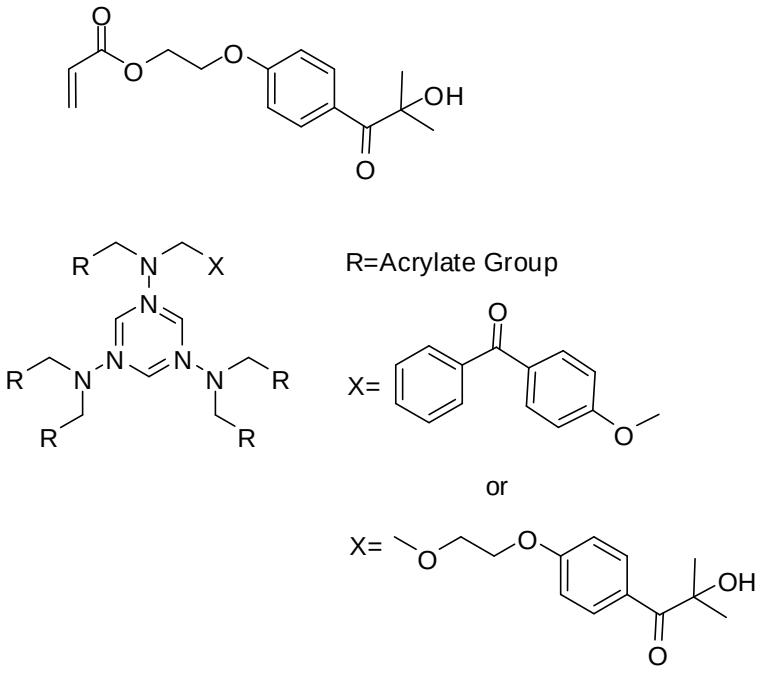

Figure 1.10. Structures of monomeric photoinitiators containing Irgacure 2959 and BP moieties [17].

Water-soluble polysiloxane BP photoinitiators with various silicon content were prepared (Figure 1.11). The water solubility of the photoinitiators, the effect of the silicon content on their triplet state lifetimes, photopolymerization properties, the self-floating

ability in the water system, and the internal connection between the surface morphology and property of the gradient polymer and film initiated by the photoinitiators were investigated [18].

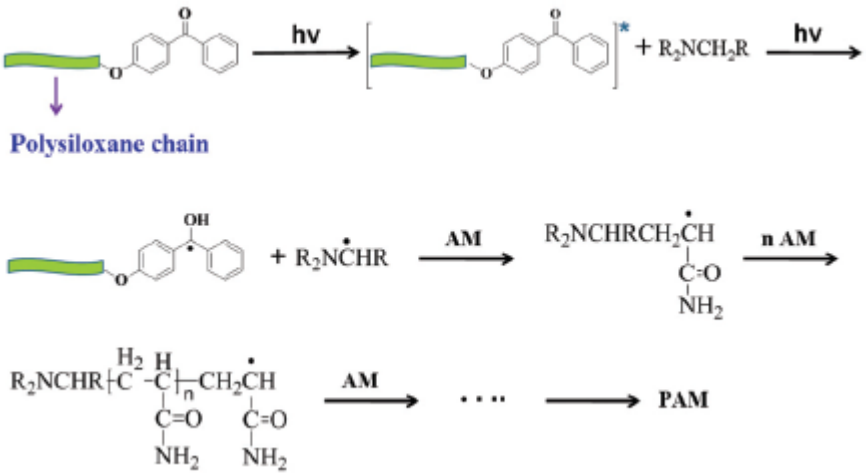

Figure 1.11. The mechanism of polymerization initiated by polysiloxane-modified photoinitiators [18].

TXs are among one of the well-known Type-II photoinitiators in photopolymerization reactions [4, 19]. They can be incorporated to polymers using different methods. 1,3-dipolar azide-alkyne [3+2] and thermoreversible Diels-Alder [4+2] click reactions were combined to synthesize polymers bearing side-chain TX photoactive groups (Figure 1.12) [6].

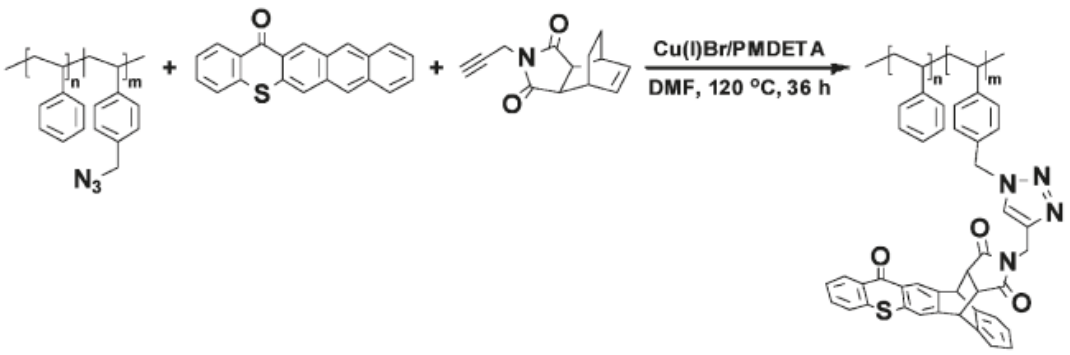

Figure 1.12. Polymeric TX photoinitiators synthesized by click reaction [6].

Photoinitiators containing both Type II photoinitiators and coinitiator in the same macromolecule were synthesized to prevent unreacted low molecular weight coinitiator residues [18-29]:

The combination of both BP derivatives and coinitiator amine into the same polymer chain has clear advantages such as intramolecular reactions responsible for the generation of more reactive species, as a consequence of the polymer effect. Macrophotoinitiators synthesized by step polymerization of BP and different coinitiator amino monomers showed that the efficiency of the photopolymerization is mainly affected by structure of amine in polymeric chain [20] (Figure 1.13).

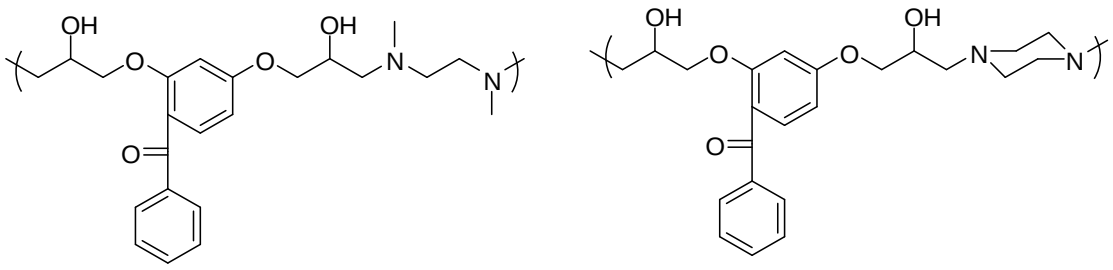

Figure 1.13. PPIs containing in-chain BP and amine [20].

PPIs containing in-chain BP and coinitiator amine were synthesized through polycondensation of toluene-2,4-diisocyanate and different BP-containing amines and the results indicated that the efficiency of polymeric initiators containing in-chain BP is different from that of the side-chain ones [21].

The efficiency of one-component polymeric BP photoinitiator containing poly(ethylene glycol), with different molecular weight, as hydrogen donor was examined. PEG-BP was found to have better water solubility than BP (Figure 1.14). The obvious advantage of this initiator is the elimination of amine based hydrogen donors and to provide alternative hydrogen donors with easily availability and non-toxicity [22].

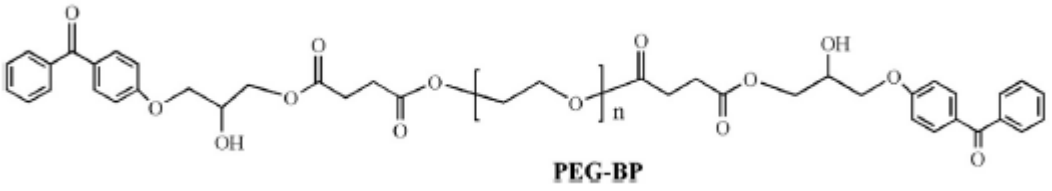

Figure 1.14. The structure of PEG-BP photoinitiator [22].

Sulfur-containing PPIs with side-chain BP and coinitiator amine were synthesized to compare the photoefficiencies of PPIs with their corresponding monomeric analogs (Figure 1.15) [23-25]. The copolymeric photoinitiator was found to be most efficient photoinitiator system compared to monomeric amine and BP/amine systems. Besides, these macrophotoinitiators showed increased photoefficiency from the photolysis reaction of the C-S bond [23].

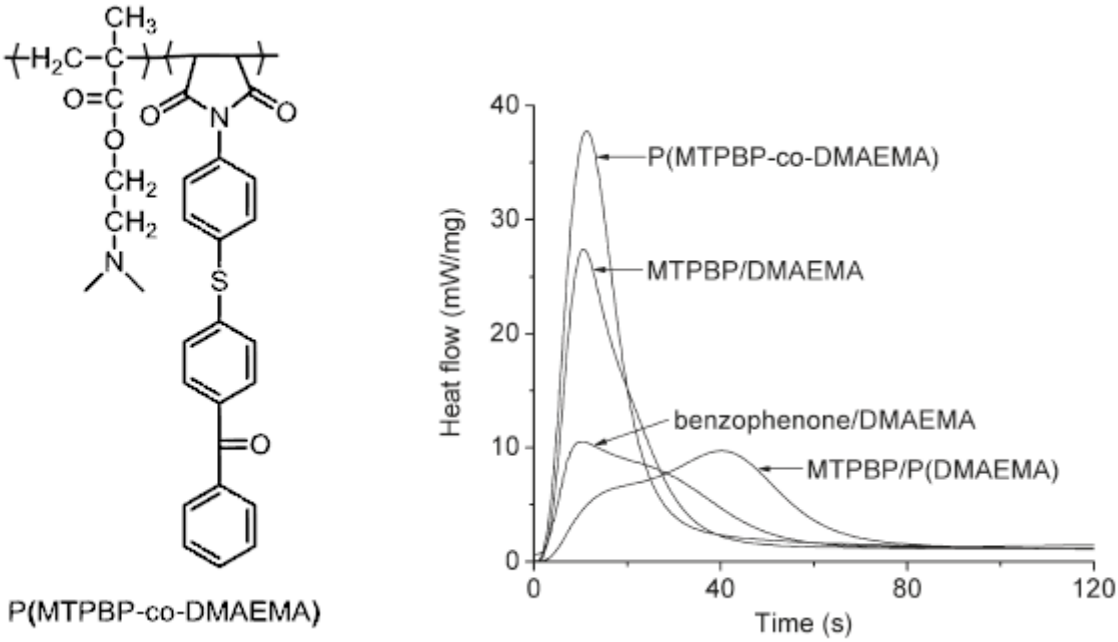

Figure 1.15. Structure of a sulfur-containing PPI with side-chain BP groups [23].

The photosensitive BP group covalently attached to the side chain of an alkyl α-hydroxymethacrylate (RHMA) polymer in combination with low molecular weight tertiary amine resulted in photopolymerization of TEGDMA and HDDA with a higher rate of polymerization compared to all low molecular weight combinations (monomeric

photoinitiator and BP with low molecular weight amine) (Figure 1.16). Higher efficiency of the polymeric initiator were attributed to the improvement of compatibility and the polymeric effect [26].

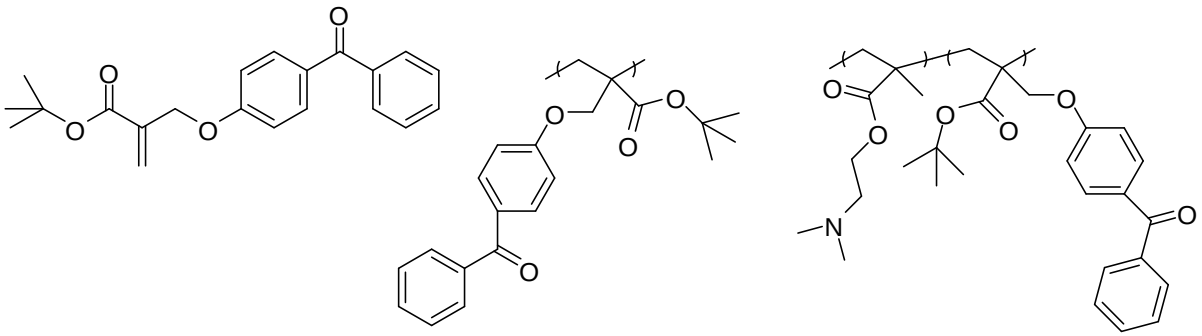

Figure 1.16. BP-containing RHMA based photoinitiators [26].

A polymeric photoinitiator (PTXP) containing in-chain TX and coinitiator amines was synthesized by step-growth polymerization (Figure 1.17). Photopolymerizations of methyl methacrylate initiated by this photoinitiator system was studied. Compared with corresponding low-molecular-weight model compounds, PTXP has a similar UV-vis spectrum with a red-shifted maximum absorption, weaker fluorescence emission, and can photoinitiate the polymerization of MMA more effectively [27].

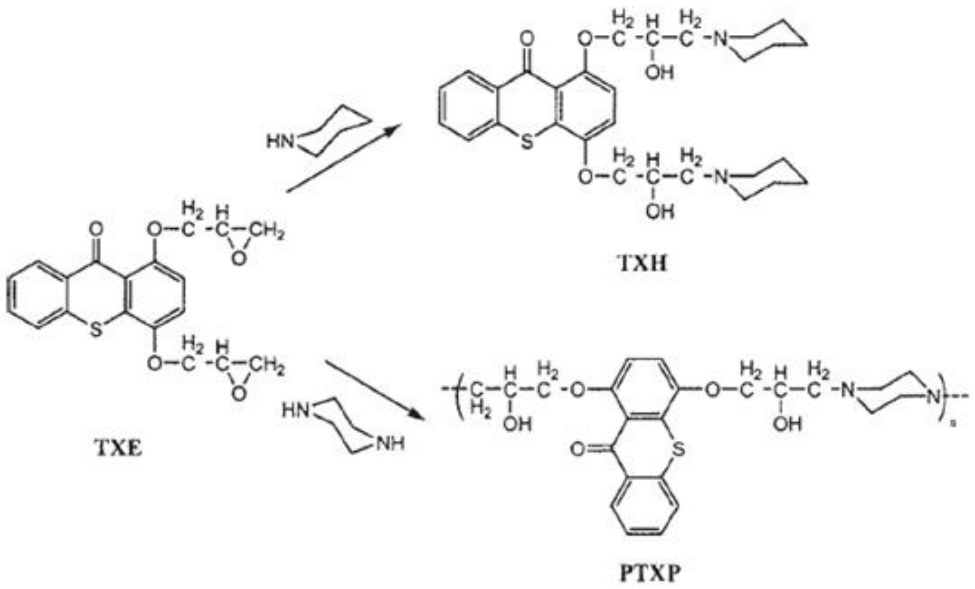

Figure 1.17. Synthesis of TX-containing PPIs [27].

A novel multifunctional photoinitiating system, self-initiated photoinitiator-monomer (photoinimer), has been synthesized to efficiently initiate polymerization of acrylates and methacrylates (Figure 1.18) [29].

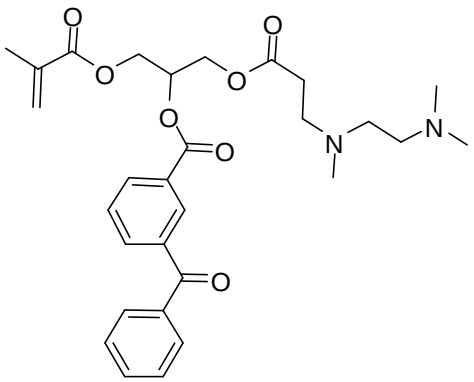

Figure 1.18. Structure of a photoinimer [29].

UV cure of pigmented coatings is a problem due to strong absorption of pigments below 380 nm. Photoinitiators such as TXs with absorptions over 380 nm are required. However, then the presence of amines causes yellowing. To solve this problem a copolymeric photoinitiator, based on side-chain TX and α-morpholino-acetophenone groups was prepared. TX is a photosensitizer absorbing over 380 nm, and can transfer the excitation energy to the other photoinitiator, promoting the free radical polymerization (Figure 1.19). Here, both PI and photosensitizers are forced to be close to each other so energy transfer is favored [30]. Similar behavior was found with other PPIs bearing side-chain TX and α-aminoacetophenone moieties [31].

The photochemistry and photoinitiation activity of a wide series of anthraquinone derivatives have been examined and compared with corresponding anthraquinone monomers (Figure 1.20). Copolymers of 2-substituted acrylamidoanthraquinone (AAAQ) and acryloxyanthraquinone (AOAQ) with methyl methacrylate have been prepared. Generally, low photoreduction quantum yields were found for the model and copolymer anthraquinones. Acryloxy copolymers exhibited higher photoreduction quantum yields than those of acrylamide anthraquinones [4].

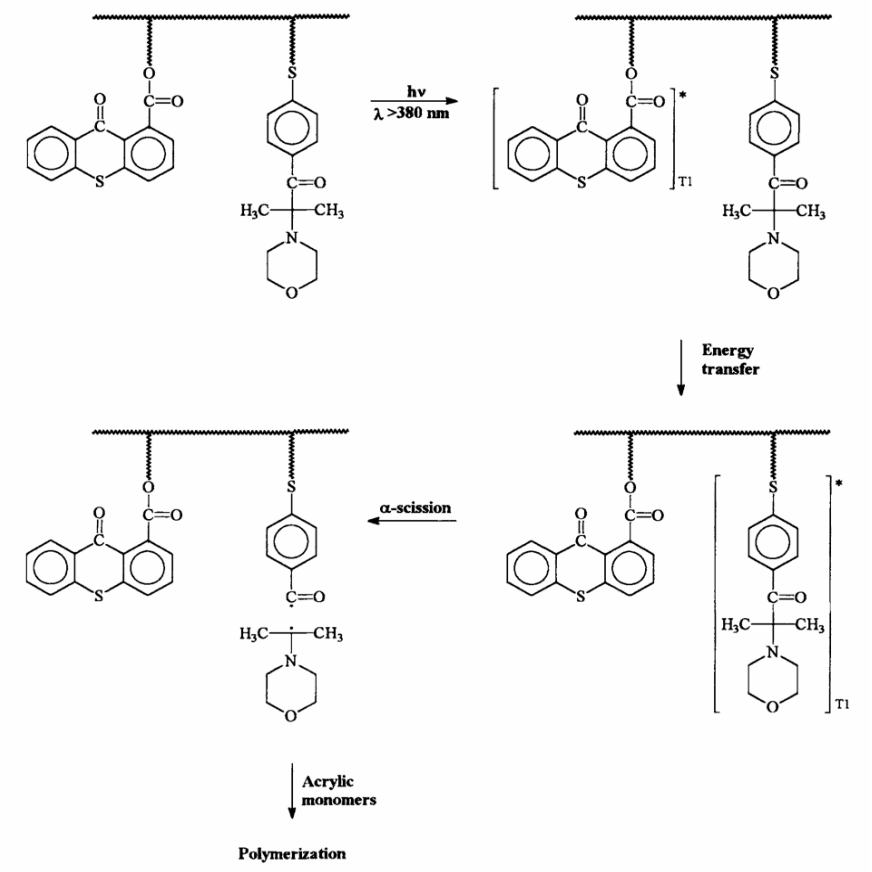

Figure 1.19. The representation of the intramolecular excitation energy transfer from the TX triplet state to the ground state α-morpholino-acetophenone chromophore [30].

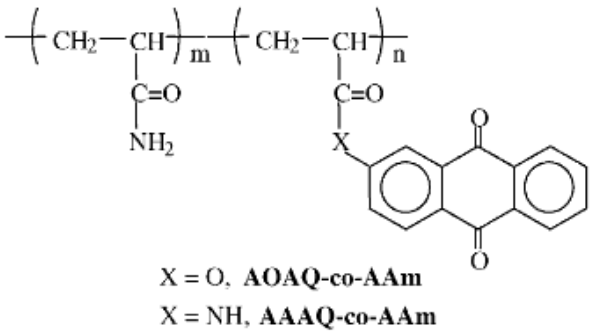

Figure 1.20. Examples of PPIs of *Type II* [4].

A polymeric initiator containing both camphorquinone and amine groups in the side chain showed lower reactivity compared to those in which only one of the photoreactive

moieties is in the polymeric form, particularly the camphorquinone group (Figure 1.21) [32-33].

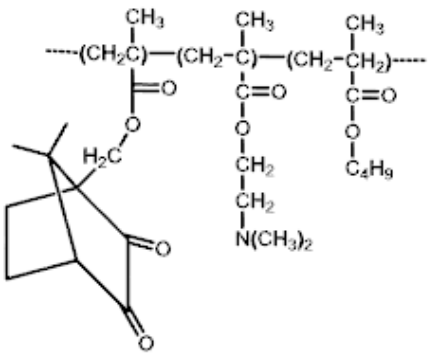

Figure 1.21. Structure of a camphorquinone-based polymeric photoinitiator [32].

Photoinitiators derived from hyperbranched polymers and dendrimers have gained extensive interest in recent decades for their unique features, such as their high functionality and low viscosity compared to linear polymers.

Hyperbranched PPIs and photo coinitiators (PPCs) with multiple BP moieties has been synthesized via the acid-catalyzed esterification of hyperbranched polyglycerol (Figure 1.22). They exhibited higher photoactivity in the usual radiation-curable formulations than the corresponding low molecular weight monomeric photoinitiators. Moreover, low viscosity and low extractability after curing made the resulting hyperbranched PPIs and PPCs appealing as components in inks for inkjet printing, or in food packaging [34].

The thiol-ene click chemistry has drawn great attention for its unique merits [35]. Sulfur atom in photoinitiators may lead to obvious red shift in the UV-vis spectra. Besides, they may undergo photolysis reaction at the C-S bond as that in Type I photoinitiators, aside from H-abstraction reaction [36]; which would greatly enhance photoinitiating efficiency.

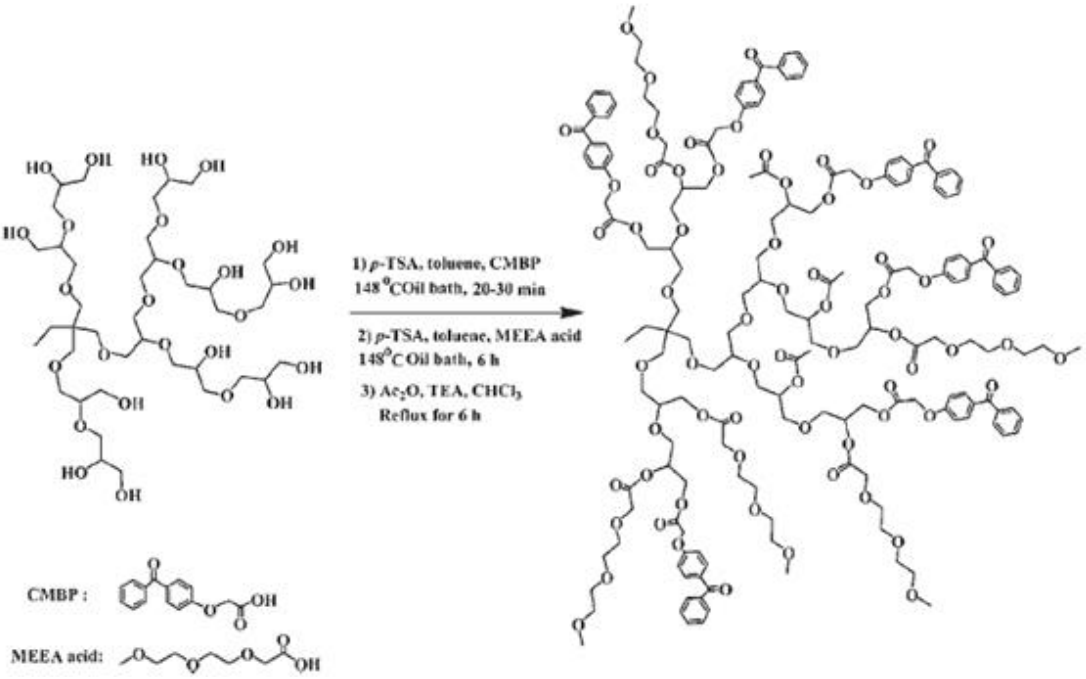

Figure 1.22. Synthesis of multifunctional hyperbranched PPIs [34].

A series of novel hyperbranched PPIs via Michael addition and thiol-ene click reaction were synthesized. They possess much stronger absorption at 340 nm and remerkable red shift from ~250 to ~280 nm when compared with BP in UV-vis spectra. They also exhibited high photoinitiating efficiency and good compatibility in the resin (Figure 1.23) [37].

A new class of hyperbranched PPIs with built-in amine coinitiators (Figure 1.24) has been developed, showing high functionality, low viscosity, good compatibility with the usual radiation curable formulations, high photoactivity and low extractability from the cured sample [38].

UV-sensitive, hyperbranched-poly(siloxysilane)-based PPIs, bearing an alkyl moiety linked to the surface of a hyperbranched polymer were synthesized via the hydrosilylation of hyperbranched poly(siloxysilane) and modified UV-sensitive compounds [39]. The UV-curing behaviors of the blends of the hyperbranched PPIs with UV-curable epoxy acrylate (EA) resin were determined and the results showed that the initiation efficiency of the PPIs

was excellent and the thermostability of the EA /polymeric photoinitiator curing systems was higher than that of the EA/PIs [39].

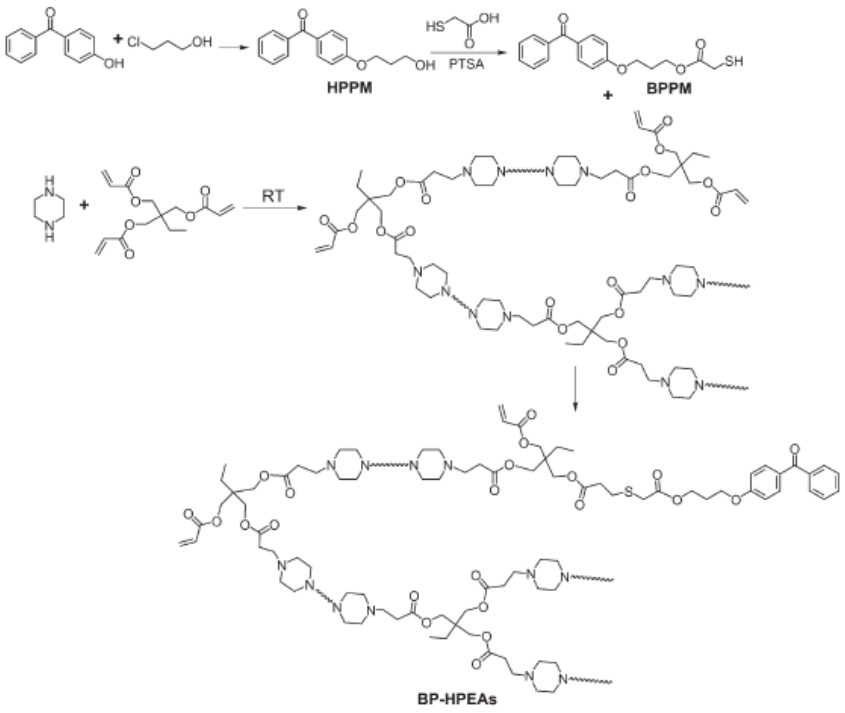

Figure 1.23. Synthesis of a photoinitiator containing BP with built-in tertiary amine from trimethylolpropanetriacrylate [37].

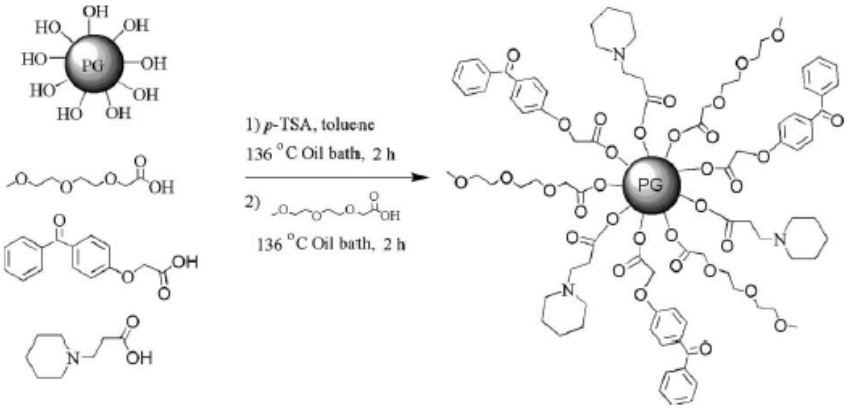

Figure 1.24. Synthesis of hyperbranched PPI with built-in aliphatic tertiary amine coinitiator [38].

Amphipathic hyperbranched polymeric TX photoinitiators (AHPTXs) were synthesized by introducing TX and polyethylene glycol monoethylether glycidyl ether into periphery of hyperbranched poly(ethylene imine), as well as low molecular weight analogue TX (Figure 1.25) [40]. AHPTXs possess UV-vis absorption spectra similar to TX derivatives, and weaker fluorescence emission in comparison to low-molecular weight analogues. AHPTXs can not be only dispersed easily in many solvents and acrylate monomers, but also are soluble in water. They have high potential in application such as coatings, inks and photo-curing hydrogels [40].

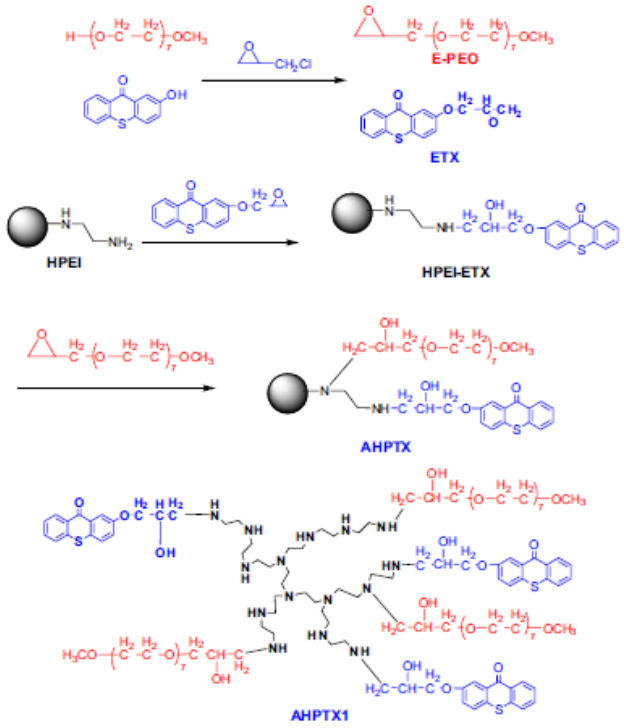

Figure 1.25. Synthesis of a hyperbranced PPI from poly(ethylene imine) [40].

1.4. Monomers

Acrylates and methacrylates hold a major place in the monomer market because of their high rates of polymerization and good chemical, optical and mechanical properties of their polymers [41]. Methacrylates are less reactive than acrylates, but are less toxic and cause less skin irritation than acrylates. On the other hand, methacrylates have some restrictions including oxygen inhibition, low polymerization rate, polymerization shrinkage

and residual unsaturation which reduces the polymer activity and lifetime [42]. Oxygen molecules in air hinder free radical photopolymerization of methacrylates by quenching radiation the excited state of initiator upon irradiation and fast scavenging of the generated radicals [43]. Photopolymerization is thus often performed under inert atmosphere such as nitrogen to prevent air from reaching the polymerization systems. Additives can be used to supress oxygen inhibition [44].

Acrylates can be monofunctional, difunctional, tri or tetrafunctional and oligomers. UV-curing of acrylate coatings is also performed in the presence of air and oxygen inhibition [45-47]. Multifunctional monomers can be used in order to enhance polymerization rate and their photopolymerization provides a method for rapid curing at room temperature to form highly crosslinked and glassy polymer networks. While the high crosslinking density of these networks increases dimensional stability and high glass transition temperatures, it decreases solvent absorption. The polymerization of multifunctional monomers features autoacceleration and network heterogeneity during the polymerization. Even though unreacted functional groups and initiator exist, a maximum functional group conversion is obtained [48]. On the other hand, an increase in monomer functionality causes residual unsaturation and crosslink density which reduces material properties because of increased brittleness. The residual unsaturation leads to toxicity problems due to leakage of monomer [49].

Crosslinking of already existing polymers is also a viable process and is currently a very active field of research. It is important to use monofunctional monomers with high rate of polymerization as reactive diluents in order for complete conversion and good polymer properties. Thus finding out the factors advancing crosslinking abilities and their reactivities are ongoing research.

1.5. Light sources

Light sources are one of the three components, apart from photoinitiators and monomers, that enable the photopolymerization process to work. A wide range of light sources is used to initiate the photopolymerization reaction.

Typical light sources are conventional artificial light sources, laser beams and the sun [50-54]. Xenon lamps, mercury arc lamps, light-emitting diodes (LEDs), laser sources are some of the commonly used light sources.

1.5.1. Xenon lamps

Xenon (Xe) as well as mercury (Hg) lamps have high electrical power needs and release a lot of heat but emit a high light intensity over a wide spectral range. For laboratory equipment, the light intensities are relatively low compared to the Xe-Hg lamp (e.g., typically 200 and ~ 60 mW cm^{-2} for Hg-Xe and Xe lamps, respectively) [9].

1.5.2. Mercury Arc Lamps

Mercury arc lamps are also commonly preferred as light sources for UV curing. They emit photons in a broad range of the electromagnetic spectrum (blue bars) as shown in Figure 1.26. Characteristic narrow transitions occur between some of the excited atomic energy levels and ground state. A set of particular wavelengths is thus emitted: 254, 313, 366, 405, 435, 546 and 579 nm. The reflector used also affects the output spectrum and can be selected for an appropriate wavelength (254 and 366 nm). The relative intensity of the different lines depends on the Hg vapor pressure [9].

One of the main problems is the heat transfer from the mercury lamp to the substrate. The resulting temperature increase can be crucial if sensitive materials (e.g., polyolefin foils) should be coated.

1.5.3. Light-Emitting Diodes (LEDs)

LEDs emit energy in the form of photons at specific wavelength range centered at 365 nm (345-385 nm) or 395 nm (380-420 nm) with an intensity about a few 10-100 mW cm^{-2}.

A UV-LED generates UV energy in an entirely different way. As an electric current passes through a semiconductor device called a diode, it emits energy in the form of

photons. The specific materials in the diode determine the wavelengths of these photons and, in the case of UV-LEDs, the output is typically in a very narrow band +/- 20 nm. The wavelength is dependent on the band gap between excited state and the ground state of the semiconductor material. The chart in Figure 1.26 below compares the output of a 395 nm, UV-LED lamp with a typical mercury-arc lamp. It is important to note the difference in intensity and wavelength of the output as both are key to understanding a UV-curing process.

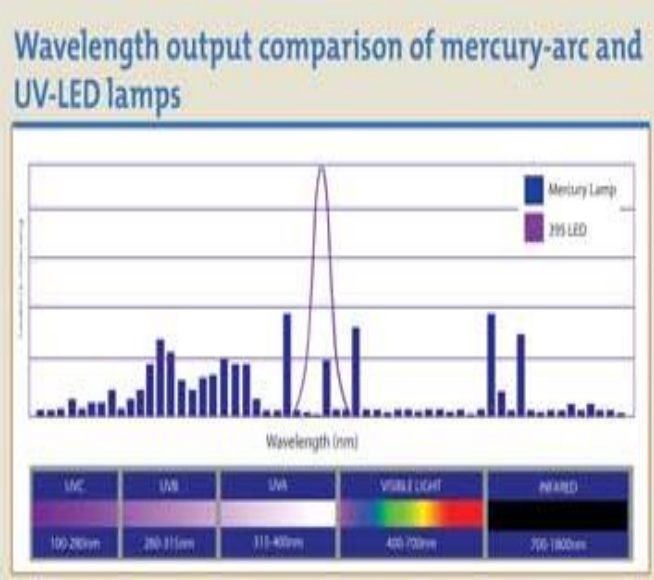

Figure 1.26. Wavelength output comparison of mercury-arc and UV-LED lamps

The main benefits of LEDs are (i) low heat generation (no IR light); (ii) low energy consumption; (iii) low operating costs, less maintenance, a ~50000 h life and portability; and (iv) a possible incorporation in programmed robots that can move the lamps to improve the curing of shadow areas. LEDs have a high potential for digital inkjet printing, adhesive curing, curing of thin heat-sensitive plastic foils, spot curing (automotive topcoat repair), and dentistry [9].

1.5.4. Laser Sources

Lasers also emit energy in the form of photons at specific wavelengths. For example argon laser emits laser lines with wavelengths that correspond to the absorption peak of

camphoroquinone, which is the initiator for dental materials. As in conventional sources, many lasers deliver the light continuously as a function of time. Some lasers can also emit the light as a (very) short pulse.

Many different lasers are available in the market; among them are the following:

(i) Continuous-wave (CW) lasers: Argon-ion lasers emitting at 488 or 514 nm appeared in the 1980s. The high power and the high quality of this light beam were beneficial for the development of many fields such as laser direct imaging (LDI), computer-to-plate (CTP) technology and holography.

(ii) Pulsed lasers: The Q-switched Nd:YAG laser could be used, however there is no strong enhancement has been detailed so far in the industry. Pulsed excimer lasers (157, 193 and 248 nm) appeared on the microelectronics market for the manufacturing of integrated circuits.

(iii) Femtosecond lasers (e.g., Ti:sapphire lasers): They have recently opened up new facilities such as two-photon stereolithography.

(iv) Semiconductor-based lasers or diode lasers: They generally emit in the red region (e.g., at 630, 680 and 720 nm) and transfer moderate light powers. At the end of the 1990s, several wavelengths were attainable in the near-UV-visible region such as at 405 nm. Diode lasers operating at selected wavelengths (405, 457, 473, 532 and 635 nm) are now available. Driving forces are basic design (no complicated laser cavity), high power output and easy stacking and adjustment (allowing the curing of complex forms) [9].

2. OBJECTIVES

Novel monomeric and polymeric photoinitiators are highly attractive due to their advantages in comparison with their corresponding low molecular weight analogues. Therefore, it is of significant interest to understand the relation between chemical structure of the monomeric/polymeric photoinitiators and their photoinitiation efficiency. This will lead to design and synthesis of novel photoinitiators with improved efficiency.

The objectives of the study are to synthesize three novel monomeric photoinitiators, bearing two identical side-chain photoinitiating groups (BP, AP or Irgacure 2959) derived from RHMA's. To date no monomer containing two photoinitiating units have been reported. Homopolymerization and copolymerization with an amine monomer gives novel polymeric photoinitiators. The photoefficiencies of each photoinitiator in the polymerizations of hexane-1,6-diol diacrylate (HDDA) is investigated using photodifferential scanning calorimeter (photo-DSC) and compared with non-bound BP, AP and Irgacure 2959.

3. EXPERIMENTAL WORK

3.1. Materials and Characterization

3.1.1. Materials

tert-Butyl α-hydroxymethacrylate (TBHMA) and CMAC were prepared according to literature procedures [55, 56].

The following analytical-grade chemicals were obtained from commercial sources and used without further purification: HDDA, BP, AP, 4-hydroxybenzophenone, 4-hydroxyacetophenone, Irgacure 2959, 2,2'-azobis(isobutyronitrile) (AIBN), DMAEM, *tert*-butyl acrylate, 1,4-Diazabicyclo[2.2.2]octane (DABCO) and all other reagents and solvents were obtained from Aldrich Chemical Co.; paraformaldehyde, sodium sulfate and thionyl chloride from Merck. Tetrahydrofuran (THF) (Merck) and triethyl amine (TEA) (Merck) were dried over activated molecular sieves.

3.1.2. Characterization

^{1}H and ^{13}C-NMR spectra were obtained on a Varian Gemini (400 MHz) spectrometer. Photopolymerizations were performed using a TA Instruments Q100 differential photocalorimeter (DPC). The glass transition temperatures were also obtained using the same instrument, under nitrogen atmosphere at a heating rate of 10 °C/min. Gel permeation chromatography (GPC) was performed on a Viscotek GPC Instrument equipped with a refractive index detector, using THF as the solvent and poly-styrene standards for calibration. The UV-Vis spectra were obtained by using a Shimadzu UV-2450 spectrophotometer. A Nicolet 6700 FT-IR spectrophotometer was used for recording IR spectra. Thermogravimetric analysis (TGA) was carried out using a TA Instrument Q50 thermogravimetric analyzer with a heating rate of 10 °C/min from room temperature to 700 °C under nitrogen purge.

3.2. Synthesis of Monomeric Photoinitiators

3.2.1. Synthesis of PI1

To an ice-cold solution of 4-hydroxybenzophenone (2.85 g, 14.39 mmol) and TEA (1.45 g, 14.39 mmol) in 7 mL of dry THF under a stream of nitrogen, CMAC (1.00 g, 7.19 mmol) was added dropwise. After stirring at 0 °C for 1 h and then at 55 °C for 12 h, the mixture was diluted with 50 mL of CH_2Cl_2 and extracted with distilled water (3 x 25 mL) and 1 wt% NaOH (2 x 10 mL). The organic phase was dried over anhydrous sodium sulfate, filtered and evaporated under reduced pressure. The residue was purified by recrystallization from methanol to give PI**1** as a white solid in 43 % yield (mp= 124-126 °C).

^{1}H-NMR (400 MHz, $CDCl_3$, TMS): δ = 4.92 (2H, s, CH_2O), 6.24, 6.69 (2H, s, CH_2=C), 7.01 (2H, d, Ar-CH), 7.22 (2H, d, Ar-CH), 7.26-7.70 (14H, m, Ar-CH) ppm.

^{13}C-NMR (400 MHz, $CDCl_3$, TMS): δ = 66.06 (CH_2-O), 114.33, 121.49, 128.22, 128.36 (Ar-CH), 129.75 (C=*C*H_2), 129.95, 130.86 (Ar-CH), 131.73 (Ar-C), 132.01, 132.54, 132.59 (Ar-CH), 134.71, 135.36, 137.41 (Ar-C), 138.10 (*C*=CH_2), 153.59 (Ar-C), 161.65 (Ar-C), 163.21 (C=O ester), 195.45 (C=O ketone) ppm.

FTIR (ATR): 3051 (C-H), 1726 (C=O, ester), 1643 (C=O, ketone), 1149 (C-O) cm^{-1}.

3.2.2. Synthesis of PI2

PI**2** was synthesized using the same procedure as for PI**1** using 4-hydroxyacetophenone instead of 4-hydroxybenzophenone. The pure product was obtained as a cream-color solid after recrystallization from methanol in 34% yield (mp= 129 °C).

^{1}H-NMR (400 MHz, $CDCl_3$, TMS): δ = 2.57, 2.62 (6H, s, CH_3), 4.93 (2H, s, CH_2-O), 6.25, 6.70 (2H, s, CH_2=C), 7.02 (2H, d, Ar-CH), 7.26 (2H, d, Ar-CH), 7.96 (2H, d, Ar-CH), 8.04 (2H, d, Ar-CH) ppm.

^{13}C-NMR (400 MHz, $CDCl_3$, TMS): δ = 26.36, 26.60 (CH_3), 65.97 (CH_2-O), 114.44, 121.72 (Ar-CH), 129.33 (C=*C*H_2), 130.00, 130.62 (Ar-CH), 130.94, 134.63 (Ar-C), 134.97 (*C*=CH_2), 154.05, 161.91 (Ar-C), 163.16 (C=O ester), 196.68, 196.75 (C=O ketone) ppm.

FTIR (ATR): 2970 (C-H), 1725 (C=O, ester), 1675 (C=O, ketone), 1159 (C-O) cm^{-1}.

3.2.3. Synthesis of PI**3**

PI**3** was synthesized using the same procedure as for PI**1** using Irgacure 2959 instead of 4-hydroxybenzophenone. The pure product was obtained as a clear oil after column chromatography on silica gel 60 (70-230 mesh) using hexane initially and gradually changing to ethyl acetate as eluent.

^{1}H-NMR (400 MHz, $CDCl_3$, δ, ppm): 1.58 (12H, s, CH_3), 3.85 (2H, t, CH_2-O), 4.17 (2H, t, CH_2-O), 4.27 (2H, t, CH_2-O and 2H, s, CH_2-O), 4.51 (2H, t, CH_2-O), 5.92, 6.33 (2H, s, CH_2=C), 6.93 (4H, m, Ar-CH), 8.03 (4H, m, Ar-CH).
^{13}C-NMR (400 MHz, $CDCl_3$, δ, ppm): 28.50 (CH_3), 60.37, 62.70, 66.42, 67.46, 69.39, 75.94 (CH_2-O), 114.08, 121.72 (Ar-CH), 129.33 (C=*C*H_2), 130.00, 130.62 (Ar-CH), 130.94, 134.63 (Ar-C), 134.97 (*C*=CH_2), 154.05, 161.91 (Ar-C), 163.16 (C=O ester), 196.68 (C=O ketone).

FTIR (ATR): 3452 (OH), 2974 (C-H), 1726 (C=O, ester), 1670 (C=O, ketone), 1159 (C-O) cm^{-1}.

3.3. Synthesis of Polymeric Photoinitiators

The homopolymerizations of PI**1** and PI**2** and copolymerizations of PI**1** with DMAEM were carried out in THF, and PI**3** was bulk polymerized at 60-70 °C using AIBN as thermal initiator with standard freeze-evacuate-thaw procedures. The homopolymers of PI**1** and PI**2** were isolated by pouring the reaction mixtures into a large excess of methanol, while that of PI**3** into ether and the copolymers were purified by precipitation into petroleum ether. The polymers were filtered, dried under vacuum and stored in the dark.

3.4. Photoinitiating Activity Measurements

Photopolymerization kinetics of the synthesized photoinitiators were determined by photo-DSC. HDDA samples (3-4 mg) (i) containing 1 mol% of photoinitiators PI**1**, PI**2**, PPI**1**, PPI**2**, BP and AP with 3 mol% of DMAEM or poly-DMAEM, (ii) containing 1 mol% of photoinitiators PPI(PI**1**-*co*-DMAEM) and iii) containing 2 mol% of photoinitiators PI**3**, PPI**3** and Irgacure 2959 were irradiated at 40 °C under nitrogen with a mercury lamp (light intensity of 20 mW/cm^2). Rates of polymerization were calculated according to the formula;

$$Rate = \frac{\left(Q/_s\right)M}{n(\Delta Hp)m} \tag{1.5}$$

where Q/s is the heat flow per second, M the molar mass of the monomer, n the number of double bonds per monomer molecule, ΔH_p the heat released per mole of double bonds reacted and m the mass of monomer in the sample. The theoretical value used for ΔH_p was 13.1 kcal/mol for methacrylate double bonds [57].

4. RESULTS AND DISCUSSIONS

4.1. Synthesis of Characterization of Photoinitiators

The synthetic route for the monomers with two side-chain photoinitiating groups (PI**1**, PI**2** and PI**3**) involved three steps as indicated in Figure 4.1.

(i) Synthesis of TBHMA from *tert*-butyl acrylate via DABCO-catalyzed Baylis-Hillman reaction [55]

(ii) Conversion of TBHMA to the key intermediate, CMAC, in one step on treatment with thionyl chloride,

(iii) Reaction of CMAC with 2 equivalents of 4-hydroxybenzophenone, 4-hydroxyacetophenone or Irgacure 2959 in the presence of TEA in THF at 60 °C. In the final step of this reaction, CMAC allowed incorporation of two identical photoinitiating groups via ether and ester linkages. PI**1** and PI**2** were obtained as white solids with melting points of 124-126 and 129 °C, while PI**3** was an oily liquid.

They were soluble in common organic solvents such as methylene chloride, methanol and THF but insoluble in water and hexane (Table 4.1).

Table 4.1. Solubilities of the synthesized photoinitiators in selected solvents.

Monomer/Polymer	H_2O	Methanol	Ether	CH_2Cl_2	THF	Hexane
PI**1**	-	+	-	+	+	-
PPI**1**	-	-	-	+	+	+
PPI(PI**1**-*co*-DMAEM)	-	+	-	+	+	-
PI**2**	-	+	-	+	+	-
PPI**2**	-	-	-	+	+	-
PI**3**	-	+	+	+	+	-
PPI**3**	-	+	-	+	+	-

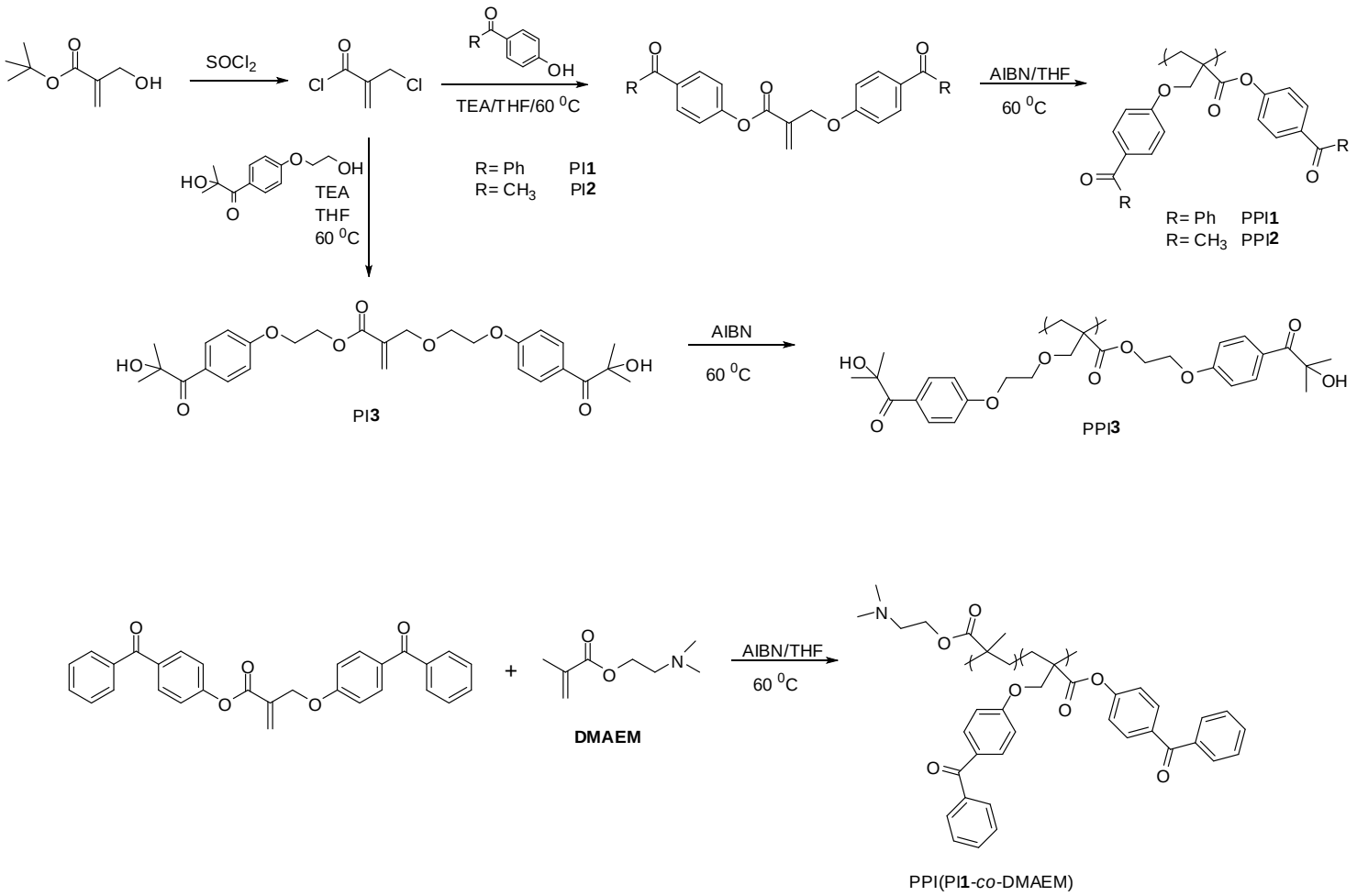

Figure 4.1. Synthesis of photoinitiators bearing two side-chain photoinitiating moieties.

FTIR, ^{1}H and ^{13}CNMR spectra of the synthesized photoinitiators were examined and found in full agreement with the proposed structures. For example, ^{1}H NMR spectrum of PI**1** showed characteristic peaks for methylene protons at 4.92 ppm, double bond protons at 6.24 and 6.69 ppm and aromatic protons between 7.0 and 7.8 ppm (Figure 4.2).

In the ^{1}H NMR spectrum of PI**2**, the two singlets seen at 2.57 and 2.62 ppm are due to two different methyl groups (Figure 4.3). ^{1}H NMR of PI**3** was also confirmed purity of this monomer (Figure 4.4). ^{13}C NMR spectra of all monomers (Figure 4.5, 4.6) show the disappearance of the methylene carbon of CMAC at 41.5 ppm (CH_2C1) and the appearance of a new oxymethylene carbon around 66 ppm. The two peaks seen around 163.0 and 196.0 ppm are typical for the C=O of ester and ketone groups. It is worth mentioning that no peaks indicating subtitution products through tertiary alcohol group of Irgacure 2959 were observed; this reaction is probably hindered by steric effects. Also, for all monomers, IR peaks due to both the ester and ketone C=O groups were observed (Figure 4.7, 4.8, 4.9).

Monomeric photoinitiators were homopolymerized under radicalic conditions to give the corresponding polymeric initiators, PPI**1**, PPI**2** and PPI**3** (Figure 4.1). PI**1** was also copolymerized in two different ratios with DMAEM (20:80 and 13:87 mol%, PI**1**:DMAEM) (Figure 4.1). Data concerning synthesis and properties of the polymers are reported in Table 4.2. The monomer concentrations of PI**1** and PI**2** were kept low during homopolymerizations to solubilize them. Solubilities of the polymers in selected solvents were given in Table 4.1. The synthesized photoinitiators have good compatibility with commercial acrylate monomers such as HDDA, 2-hydroxyethyl methacrylate, 2-hydroxyethyl acrylate and trimethylolpropane triacrylate.

IR and NMR spectra confirmed the expected structure for all the polymers. In particular, the disappearance of resonances due to the vinyl group in the NMR spectra, as well as a slight shift of carbonyl peak due to removal of conjugation in the FTIR spectra of homo-and copolymers indicated the occurrence of the polymerization reaction (Figure 4.7, Figure 4.8, Figure 4.9).

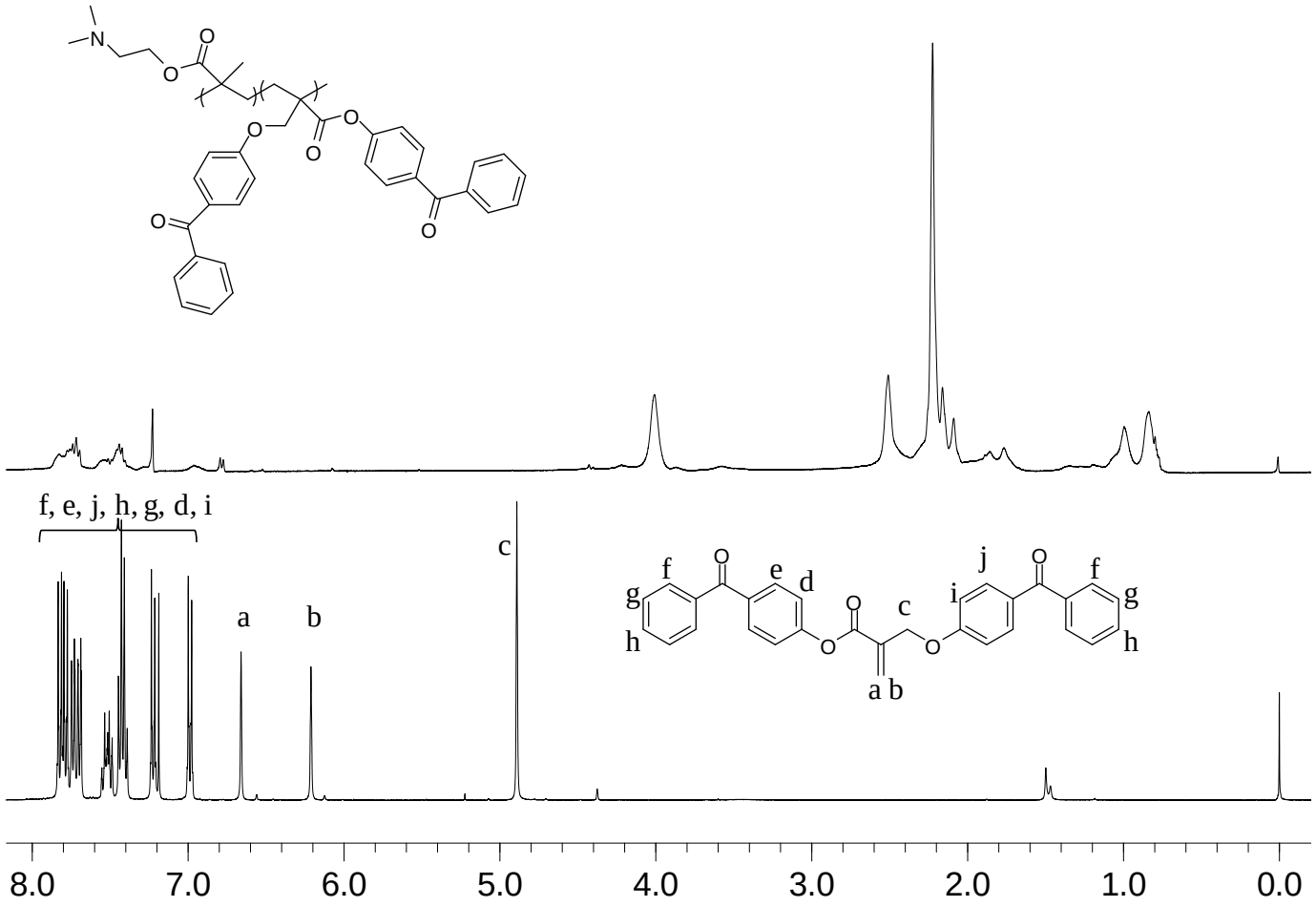

Figure 4.2. ^{1}H NMR spectra of PI**1** and PPI(PI**1**-*co*-DMAEM).

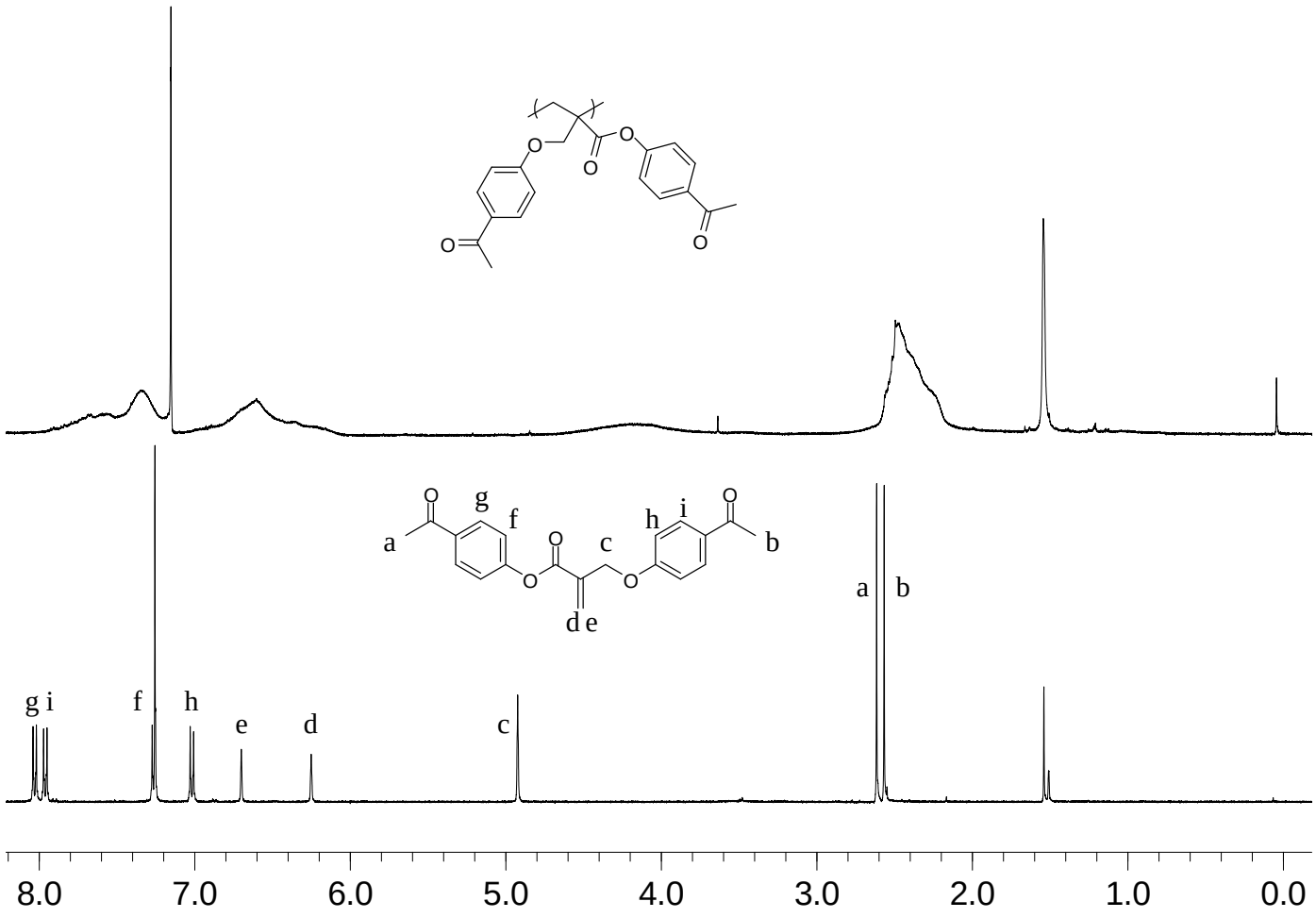

Figure 4.3. ^{1}H NMR spectra of PI**2** and PPI**2**.

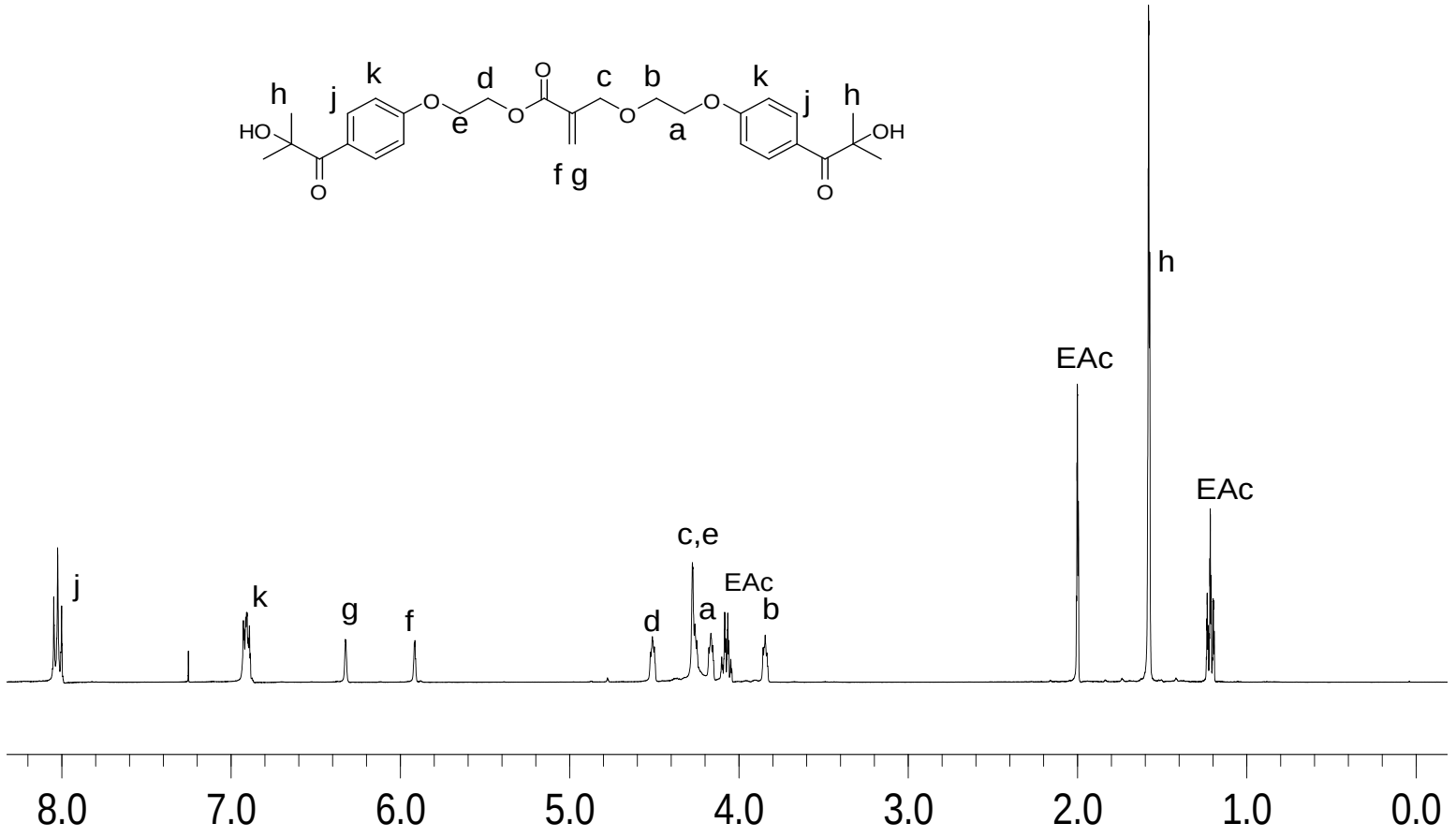

Figure 4.4. ^{1}H NMR spectrum of PI**3**.

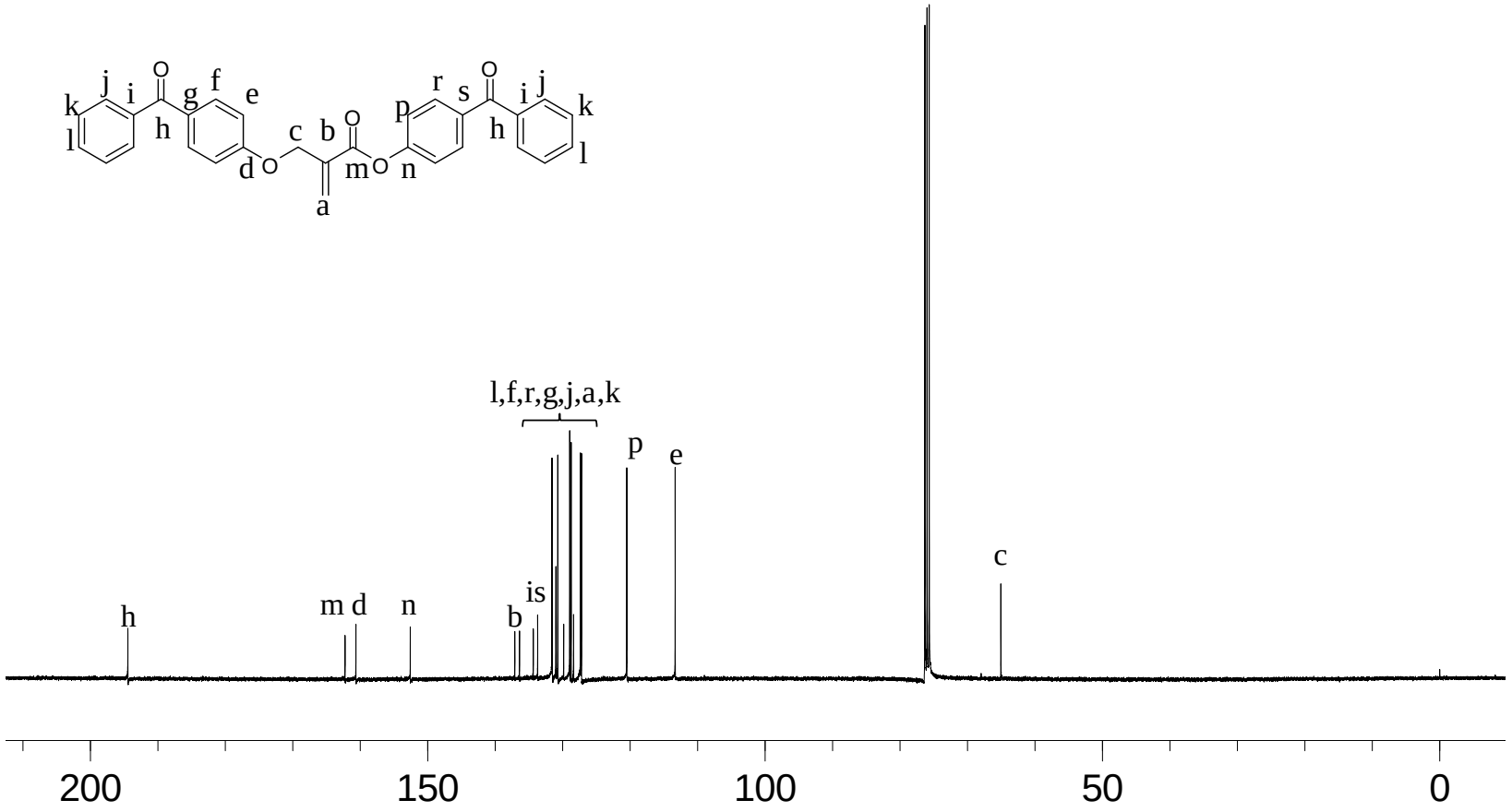

Figure 4.5. ^{13}C NMR spectrum of PI**1**.

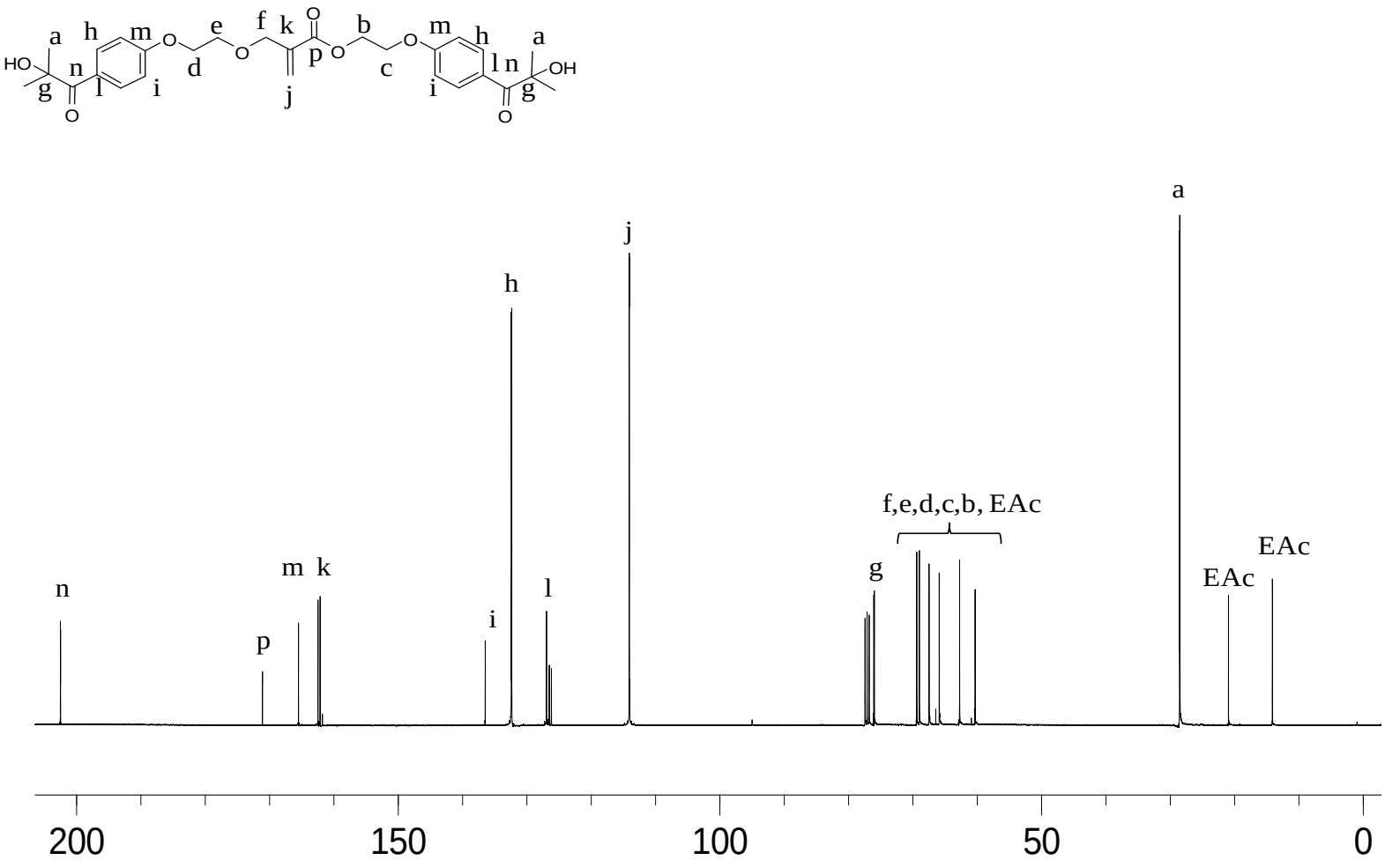

Figure 4.6. ^{13}C NMR spectrum of PI**3**.

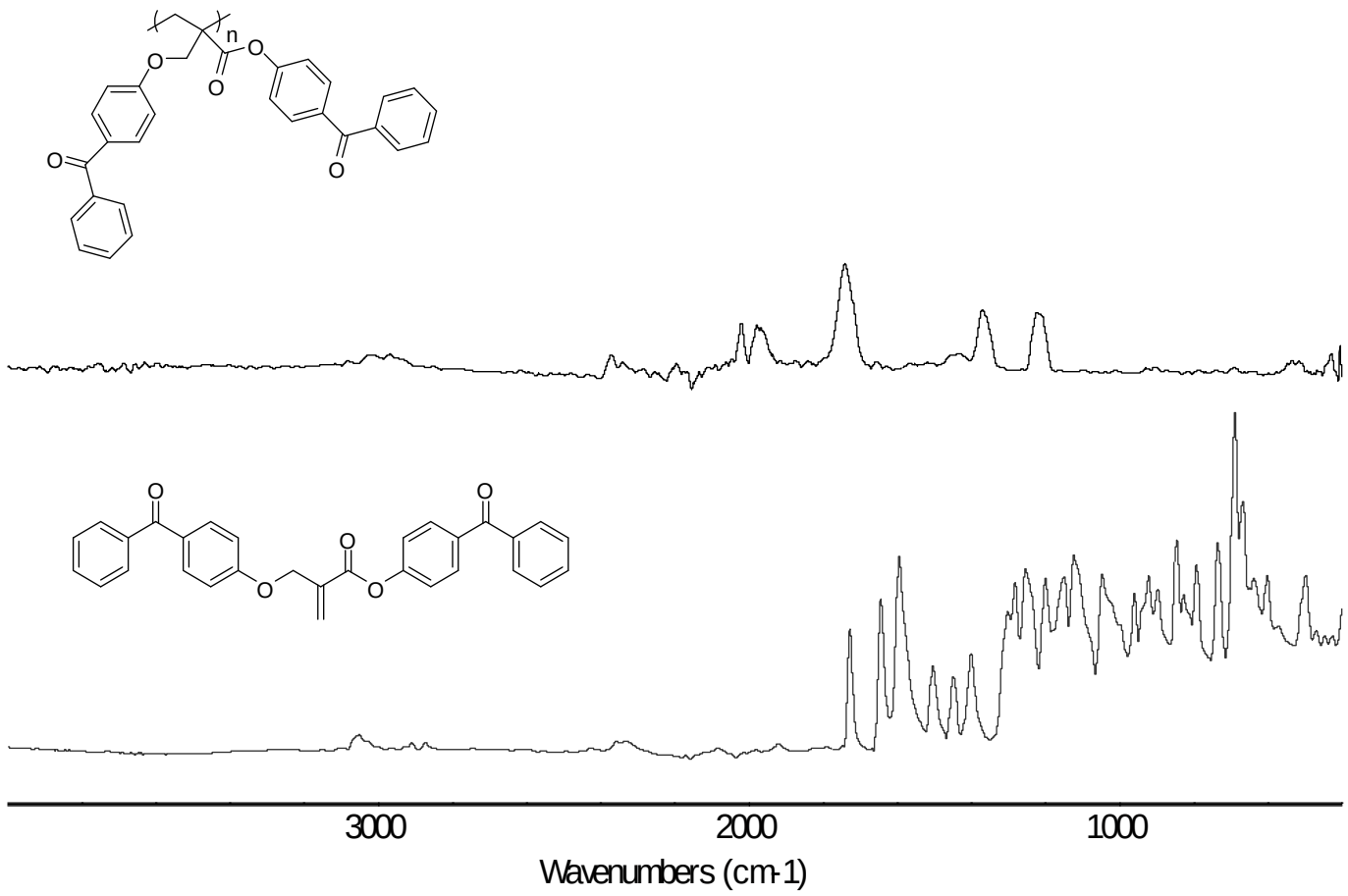

Figure 4.7. FTIR spectra of PI**1** and PPI**1**.

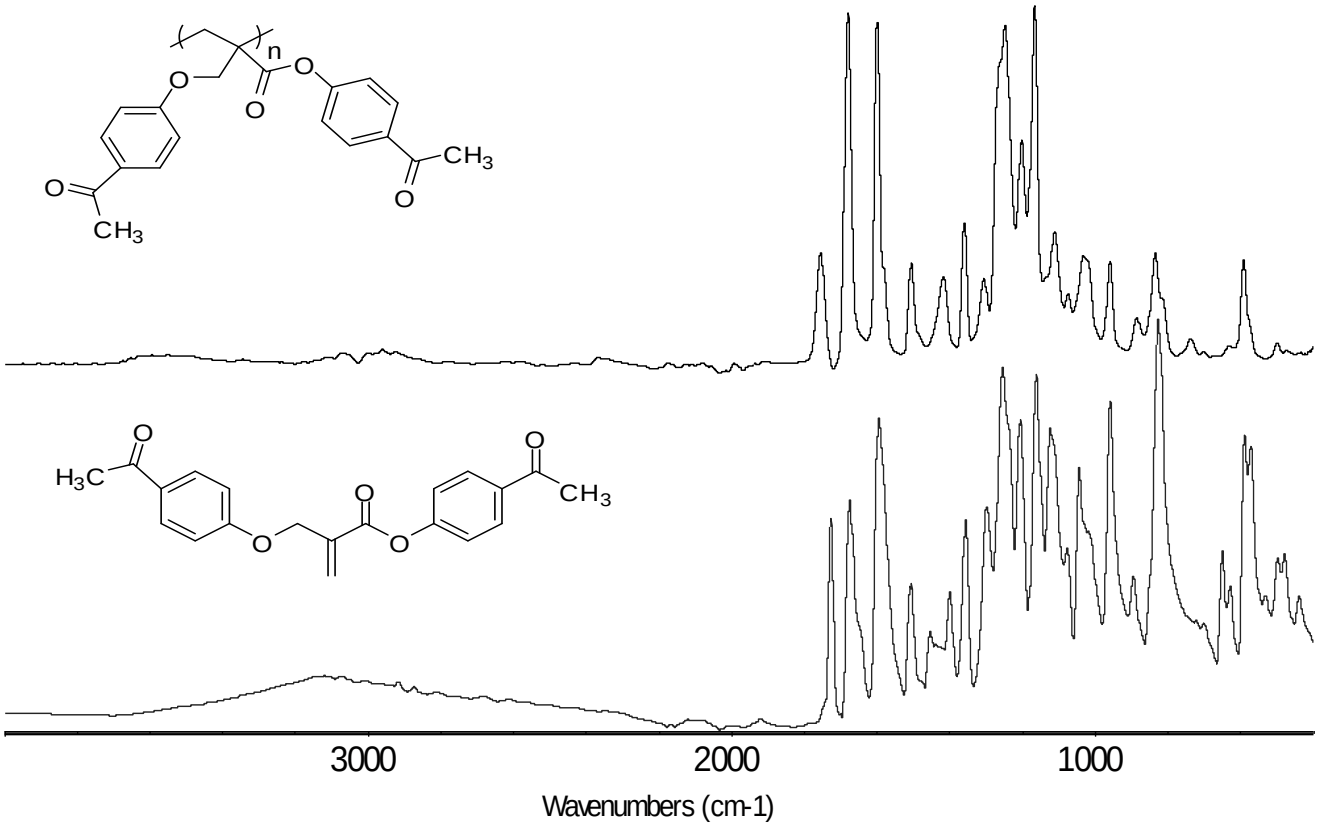

Figure 4.8. FTIR spectra of PI**2** and PPI**2**.

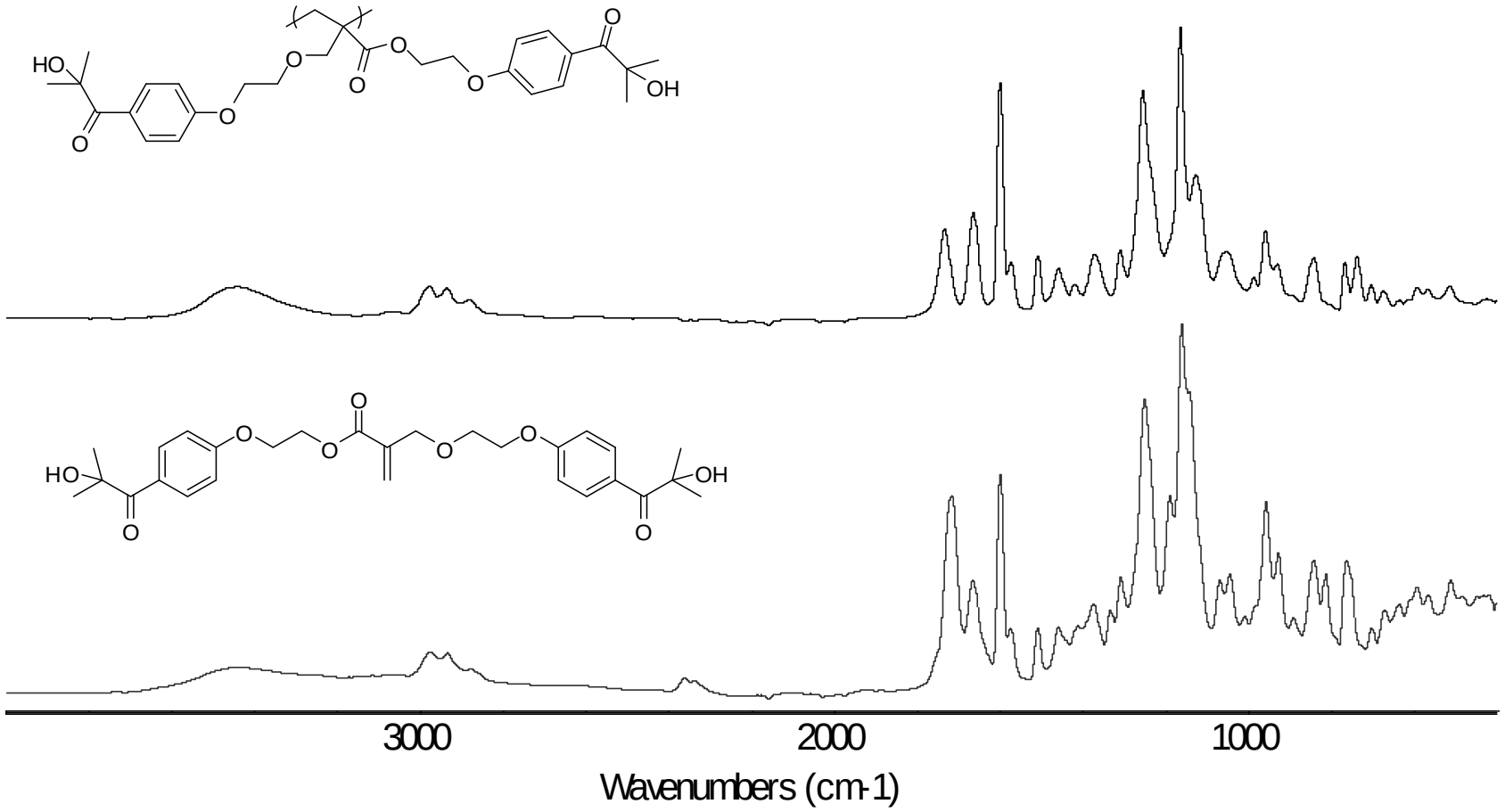

Figure 4.9. FTIR spectra of PI**3** and PPI**3**.

Table 4.2. Synthesis and characterization data for polymeric photoinitiators.

Monomer	PI in feed (mol%)	PI in copolymer (mol%)	[M]	[AIBN] x10^{-2}	Temp. (°C)	Time (h)	Yield (%)	M_n/PDI
PI**1**	100	-	0.54	1.5	70	2.5	34	3900/1.8
PI**1**	100	-	0.54	1.5	70	8.0	68	3454/1.69
DMAEM/PI**1**	13	-	8.63	1.8	60	3.0	78	-
DMAEM/PI**1**	13	12	8.63	1.8	60	2.0	52	5050/1.09
DMAEM/PI**1**	20	29	4.31	1.2	70	2.0	34	14600/1.56
DMAEM/PI**1**	20	-	4.31	1.2	70	3.5	27	-
DMAEM/PI**1**	20	-	2.87	0.9	70	3.0	60	-
PI**2**	100	-	0.53	1.7	70	23.0	34	4152/3.05
PI**2**	100	-	0.54	1.5	70	18.0	34	-
PI**3**[a]	100	-	-	2 wt%	60	24.0	20	48000/1.96

[a]bulk polymerization

Figure 4.2 shows the ^{1}H NMR spectrum of one of the copolymers of PI**1** with DMAEM. The peaks around 7-8 ppm are due to protons of BP units of PI**1**, while the peaks at 1.0, 2.2 and 2.5 ppm belong to the protons of the two different methyl and methylene groups attached to nitrogen of DMAEM; oxymethylene units of PI**1** and DMAEM overlapped around 4.0 ppm. Copolymers' composition was determined using ^{1}H NMR, by integration of aromatic protons of PI**1** with respect to oxymethylene protons of PI**1** and DMAEM (Table 4.2). As reported in Table 4.2, the copolymer compositions were similar to feed ratios, which may be due to high conversions obtained during copolymerizations (>25 %). It was not possible to evaluate the reactivity ratios of the monomers due to the same reason. The number average molecular weights (M_n) and polydispersity index (PDI) of the polymers are given in the last column of Table 4.2. The low M_n values of PPI**1** and PPI**2** can be explained by high chain transfer ability of PI**1** and PI**2** due to steric effect of two BP or AP units. The M_n values increase with an increase DMAEM units in the copolymers. The higher molecular weight of PPI**3** is due to the less bulky structure of the photoinitiating groups as well as bulk polymerization conditions.

The thermal behaviors of copolymers were investigated by DSC and TGA analysis. The DSC analysis of PPI**1**, PPI**2** and PPI**3** showed T_g values of 63, 120 and 45 °C (Figure 4.10).

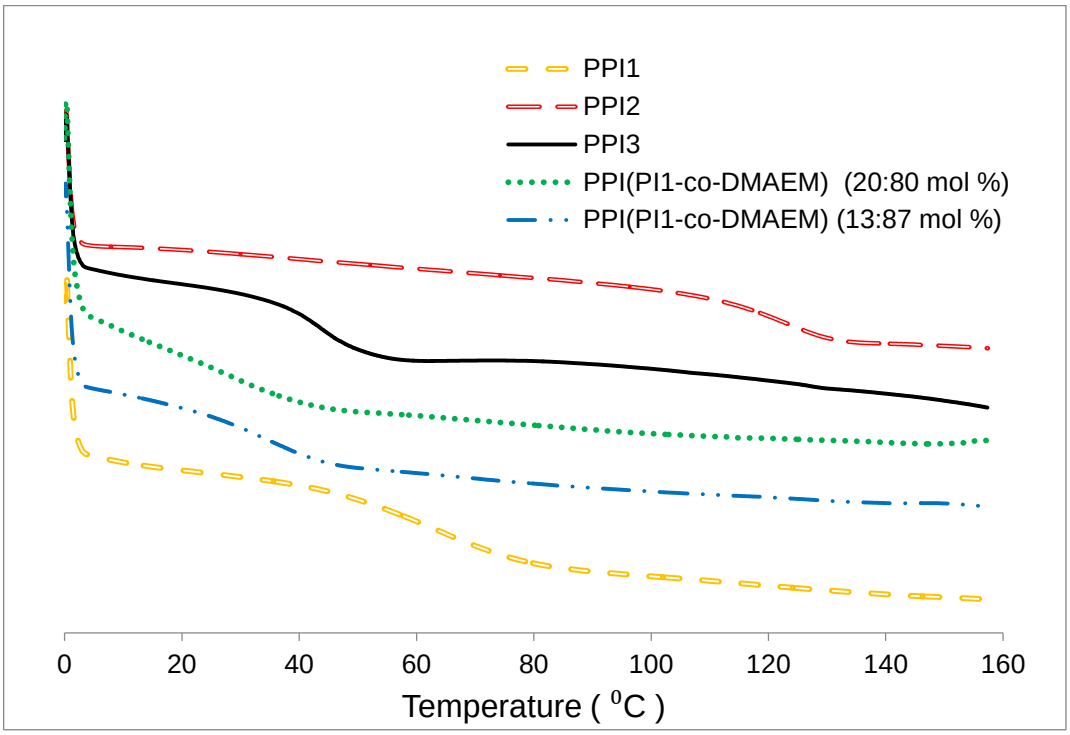

Figure 4.10. T_g analysis of polymeric photoinitiators.

It seems that the T_g values correlate well with the flexibility of the side chain of polymers, PPI**3** having the lowest value. The methyl groups of AP group on PPI**2** seem to restrict thesegmental rigidity of the polymer, thereby enhancing the T_g, more than the phenyl groups on PPI**1**. The T_g values of the copolymers were found decrease with an increase in DMAEM units in the copolymers. For example, T_g values of the copolymers (DMAEM:PI**1**, 80.0:20.0 and 87:13 mol%) were found to be 34 and 28 °C. As expected, DMAEM with a more flexible structure (T_g of poly-DMAEM is -6 °C) decreases T_g values of the copolymers.

The thermal stabilities of the homopolymers were investigated by TGA under nitrogen. The thermostability of PPI**2** and PPI**3** with a weight loss starting at about 300 °C were found to be higher than that of PPI**1** (200 °C) (Figure 4.11).

The thermal stability of the copolymers were found to be similar to PPI**1** but they undergo decomposition in two stages.

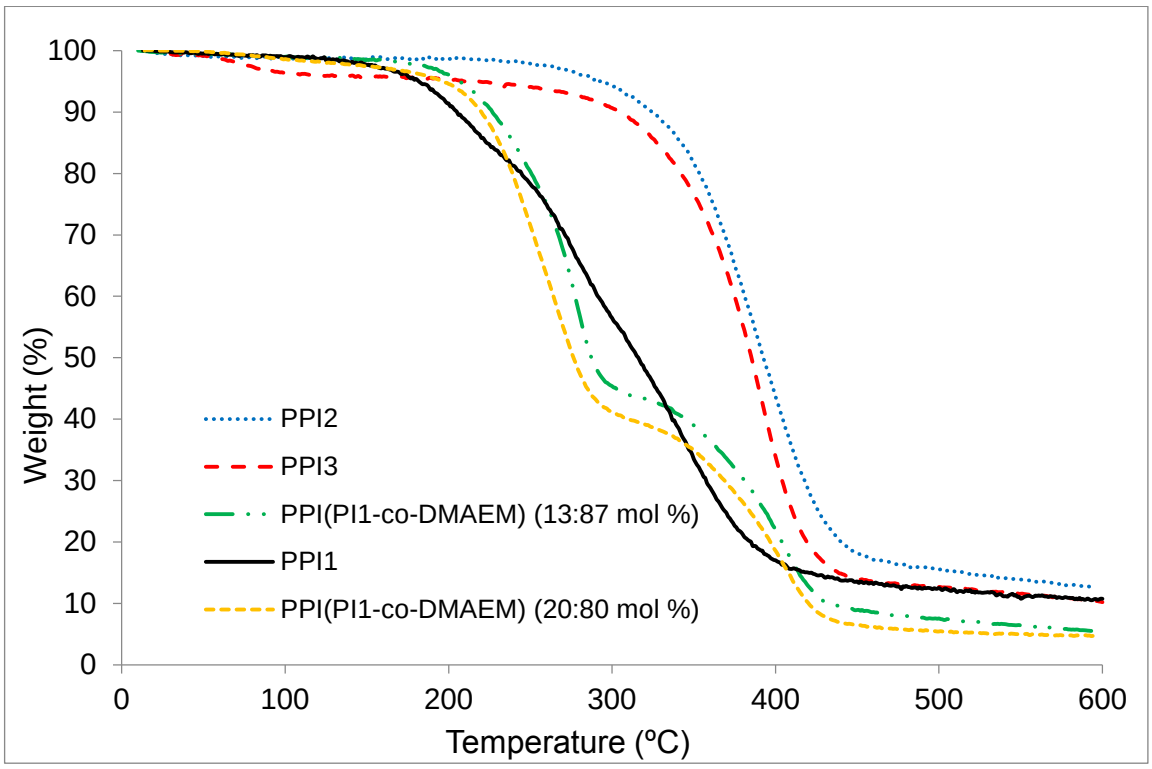

Figure 4.11. TGA traces of PPI(PI**1**-*co*-DMAEM) (20:80 mol %), PPI(PI**1**-*co*-DMAEM) (13:87 mol%), PPI**1**, PPI**2**, PPI**3.**

4.2. UV-Vis Spectral Characterization of Photoinitiators

UV-Vis absorption spectra of the synthesized photoinitiators together with BP, AP and Irgacure 2959 in chloroform were measured (Figure 4.12, Figure 4. 13). The wavelengths for maximum absorption (λ_{max}) and the values of molar extinction coefficient at λ_{max} are given in Table 4.3.

Table 4.3. Absorption properties of the synthesized photoinitiators compared with AP, BP and Irgacure 2959 in chloroform solution.

Photoinitiator	λ_{max} (nm)	ε (L mol^{-1} cm^{-1})[a]
AP	240	22353
BP	254	20676
Irgacure 2959	276	19032
PI**1**	258	9752
PI**2**	264	21655
PI**3**	276	14413
PPI**1**	262	12000
PPI**2**	256	23467
PPI**3**	272	17700
PPI(PI**1**-*co*-DMAEM) (20:80 mol%)	258	8231

[a] in terms of photoinitiating repeating units

AP and BP which are type II sensitizers, show strong π → π* absorption at 240 and 254 nm, and weak n → π* absorption at 300-350 nm. BP-containing photoinitiators PI**1**, PPI**1** and PPI(PI**1**-co-DMAEM) also exhibit strong π → π* absorption maxima at λ_{max} values similar to BP. However, their absorbance peaks are broadened toward higher wavelength so that they show enhanced absorption around 280-310 nm compared to BP. This enhancement makes polymerization feasible at longer wavelengths, equivalently, at lower photon energies.

In addition, we observed no difference in the maximum of absorption of PI**1** and PPI**1**, which indicates that polymer structure has no significant influence. AP-containing photoinitiators PI**2** and PPI**2** showed similar UV absorption spectra, which were red-shifted compared to AP. This may be ascribed to the more electron donating AP group as compared to BP. Also, the macromolecular structure has no significant influence on the absorption of AP groups. Irgacure 2959-containing photoinitiators, PI**3** and PPI**3** showed the characteristic absorption of Irgacure 2959. The extinction coefficients of the monomeric and polymeric photoinitiators were found to be similar to those of their commercial analogues.

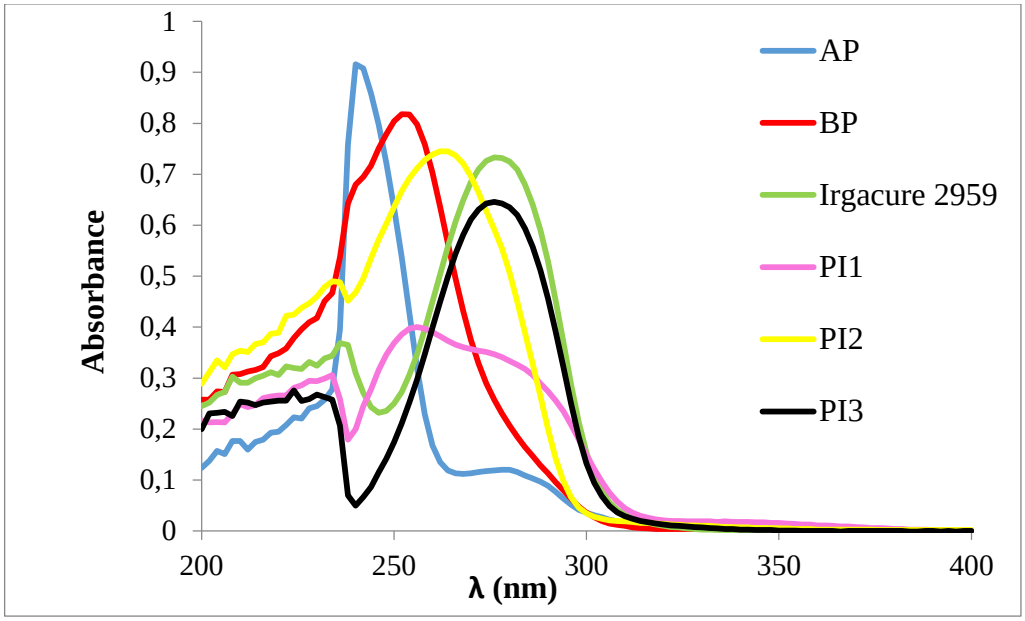

Figure 4.12. UV-Vis absorption spectra of AP, BP, Irgacure 2959, PI**1**, PI**2** and PI**3** in chloroform ($4x10^{-5}$ M) solution.

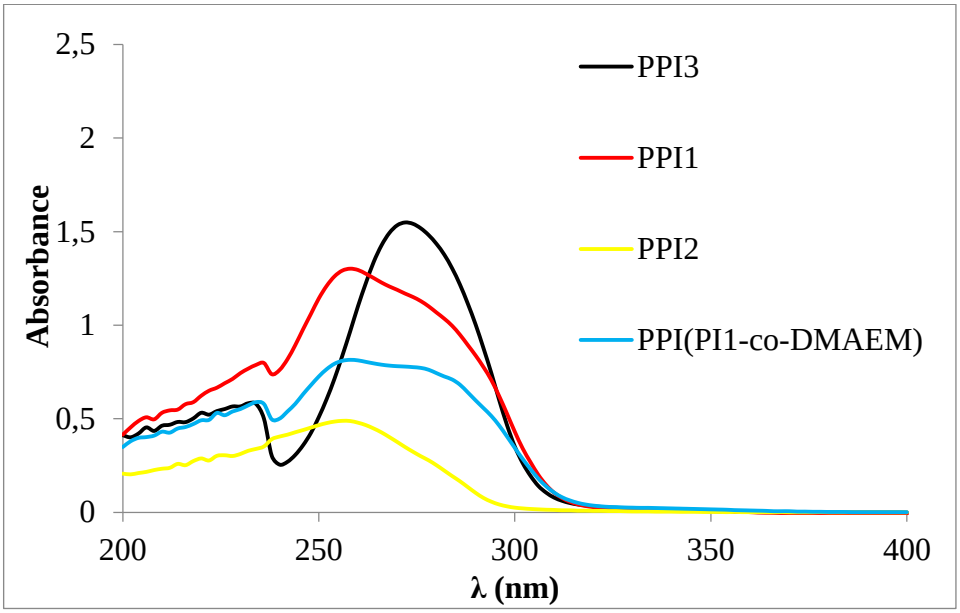

Figure 4.13. UV-Vis absorption spectra of PPI**1**, PPI**2**, PPI**3** and PPI**(**PI**1**-*co*-DMAEM) in chloroform ($4x10^{-5}$ M) solution.

4.3. Photoinitiating Activity

The photoinitiating activities of monomeric (PI**1**/DMAEM, PI**2**/DMAEM, PI**3**) and polymeric (PPI**1**/DMAEM, PPI**2**/DMAEM, PPI**3**, PPI**1**/poly-DMAEM and PPI(PI**1**-*co*-DMAEM)) photoinitiators were tested toward HDDA monomer under nitrogen atmosphere through photo-DSC. The polymerization profiles (Figure 4.14, Figure 4.15, Figure 4.16, Figure 4.17, Figure 4.18) show the maximum polymerization rate (R_{pmax}), conversion as well as the induction time. For comparison, the commercial photoinitiators BP, AP and Irgacure 2959 were also tested under the same conditions.

The photo-DSC results of type II monomeric photoinitiators (PI**1** and PI**2**) together with commercial small molecular weight photoinitiators (AP, BP) are shown in Figure 4.14. It can be easily observed that PI**1** is more efficient photoinitiator than BP, R_{pmax} value is about twice that of BP. This result may be attributed to high BP concentration in PI**1** compared to BP, where photoinitiator and amine concentrations in HDDA are 1 and 3 mol%. However, when photoinitiator concentration is halved by keeping the amine concentration same or both them are halved no significant effect on both rate of polymerization and conversion were observed (Figure 4.15). The high reactivity of PI**1** may be ascribed to its higher absorption of π - π^* transition at wavelengths around 280-310 nm. Also the system composed of PI**1** with low molecular weight amine was found to be more effective compared to the same photoinitiator with macromolecular amine. This result is probably due to the low mobility of macromolecular amine which makes proton transfer between the excited state of BP groups and DMAEM polymerization difficult. The conversions reached for PI**1**/amine systems and BP were similar and around 70%. Contrary to PI**1**/DMAEM system, PI**2**/DMAEM showed very low photopolymerization efficiency compared to AP.

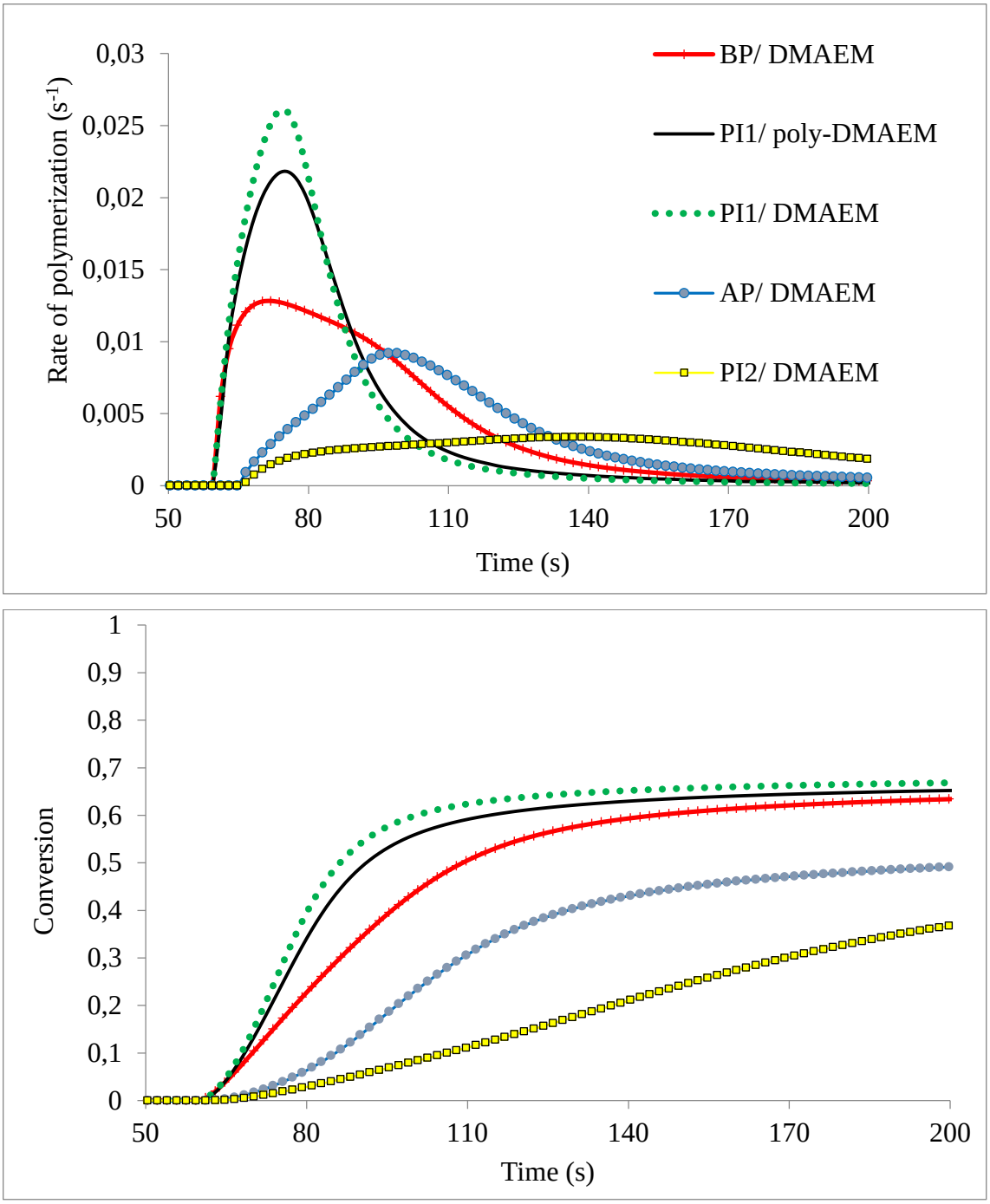

Figure 4.14. Rate-time and conversion-time plots for the photopolymerization of HDDA initiated by BP/DMAEM, PI**1**/poly-DMAEM, AP/DMAEM, PI**2**/DMAEM, PI**1**/DMAEM. Photoinitiator and amine concentration in monomer are 1 and 3 mol%.

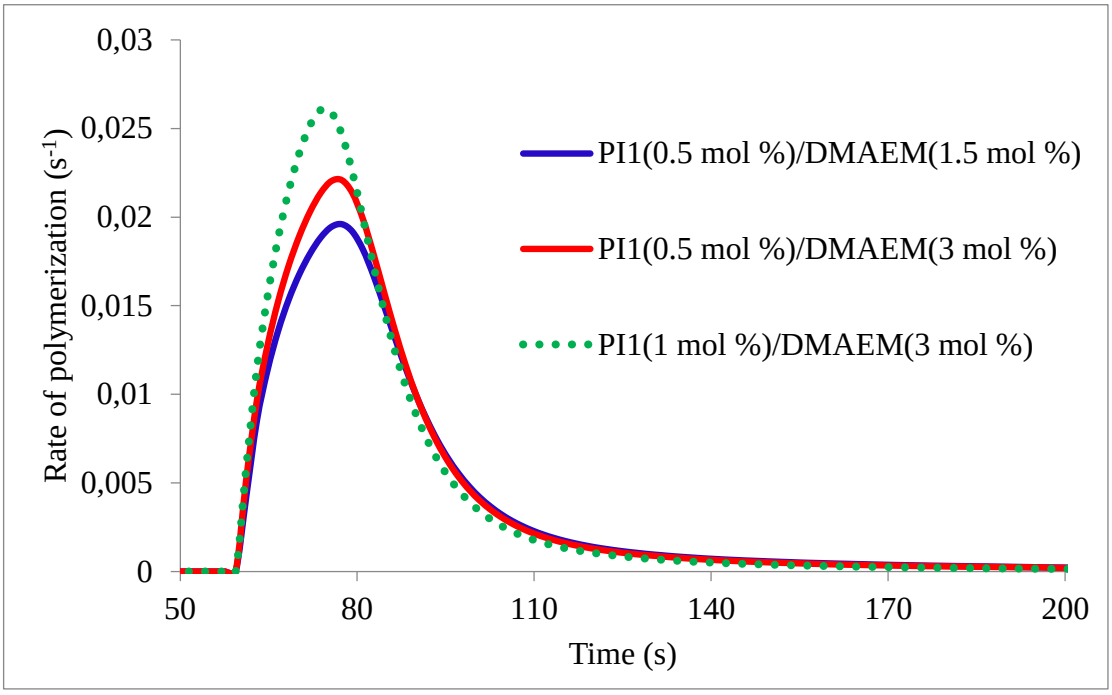

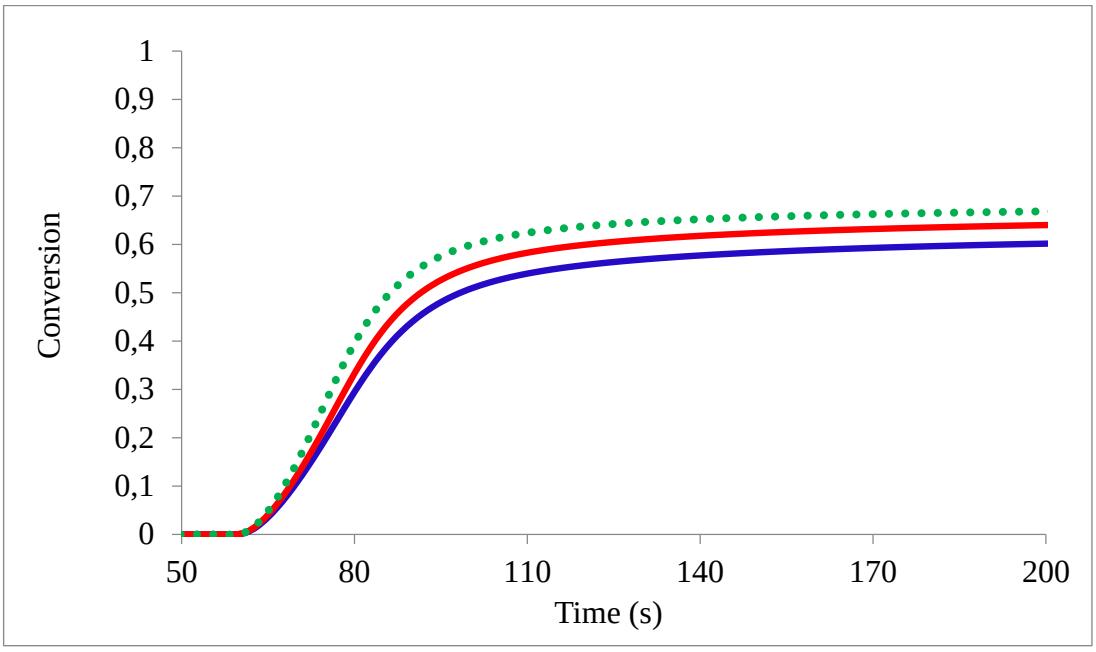

Figure 4.15. Rate-time and conversion-time plots for the photopolymerization of HDDA initiated by PI**1**(0.5 mol %)/DMAEM(1.5 mol %), PI**1**(0.5 mol %)/DMAEM(3 mol %), PI**1**(1 mol %)/DMAEM(3 mol %).

The polymeric photoinitiator PPI**1** with the low molecular weight amine was found to be even faster than PI**1**/amine pair (Figure 4.16). This result may be addressed to improved compatibility of the polymer in HDDA and also improved energy migration

along the polymer chain. However, the photoinitiating system composed of PPI**1** and the high molecular weight amine exhibits slightly lower activity, similar to PI**1**/DMAEM system due to the same reason.

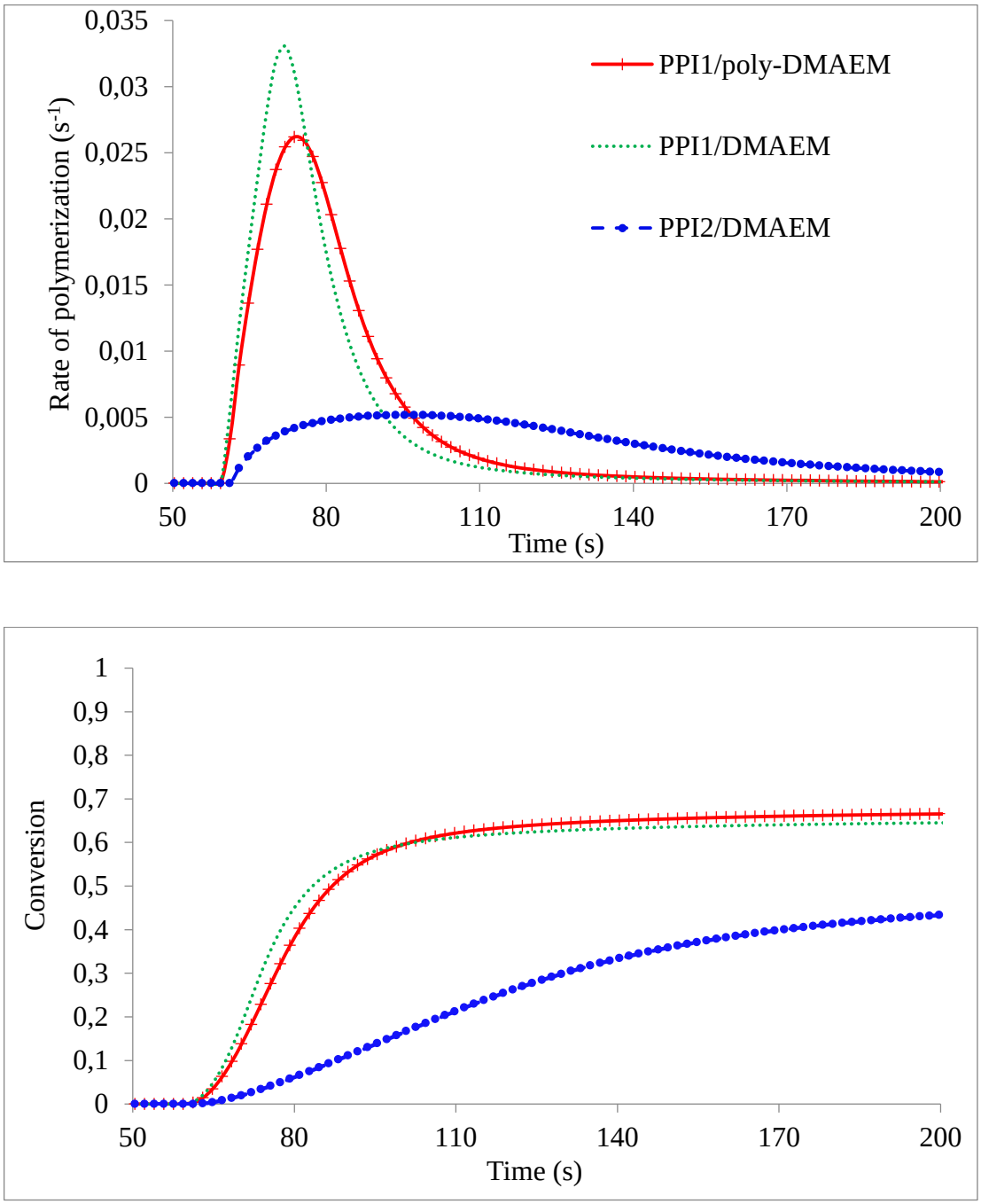

Figure 4.16. Rate-time and conversion-time plots for the photopolymerization of HDDA initiated by PPI**1**/poly-DMAEM, PPI**2**/DMAEM, PPI**1**/DMAEM. Photoinitiator and amine concentration in monomer are 1 and 3 mol%.

The copolymeric photoinitiators, PPI(PI**1**-*co*-DMAEM) in two different ratios, showed slightly lower efficiency than the monomeric (PI**1**/DMAEM) system. This is probably due to the low mobility of macromolecular amine (Figure 4.17).

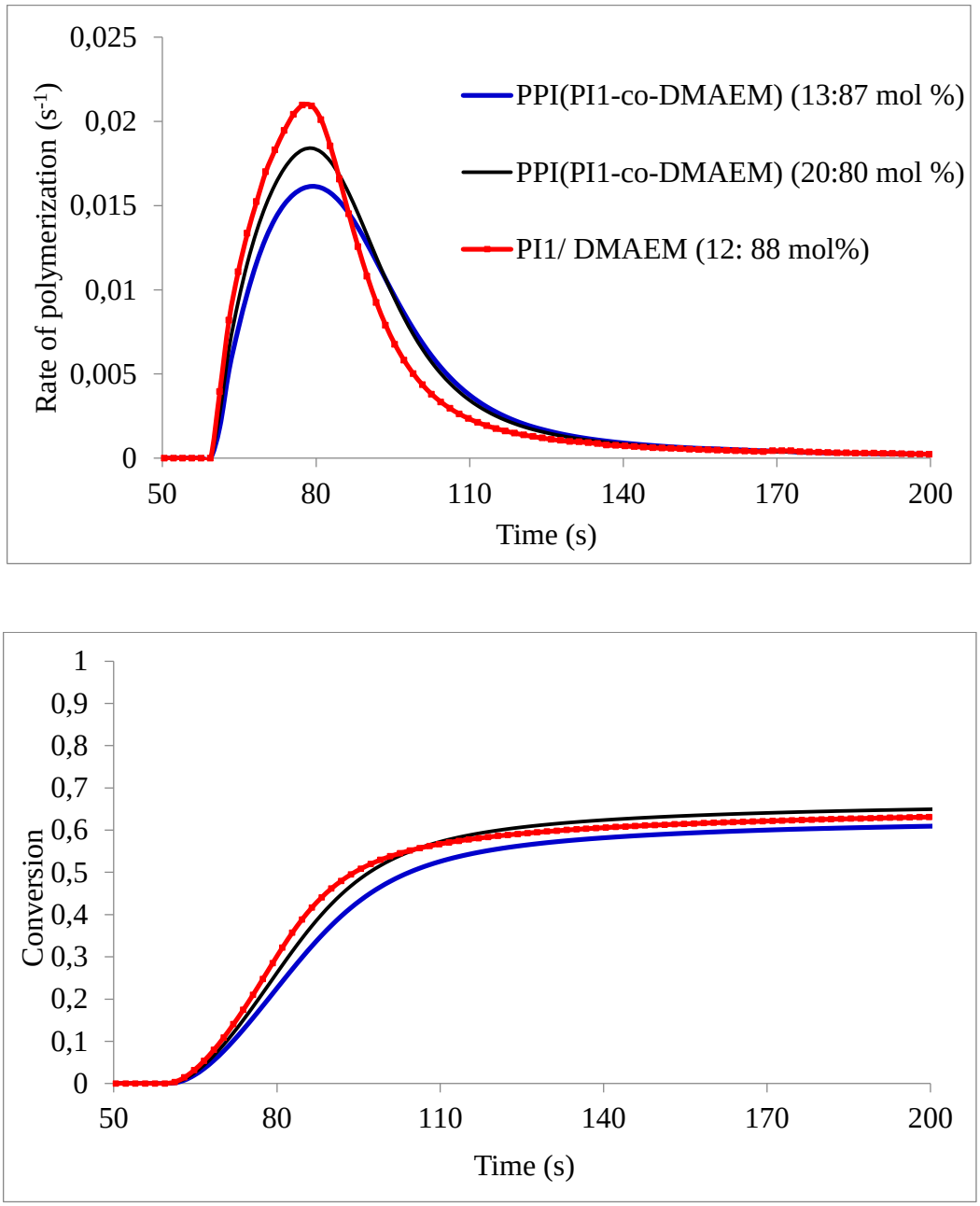

Figure 4.17. Rate-time and conversion-time plots for the photopolymerization of HDDA initiated by PPI(PI**1**-*co*-DMAEM) (13:87 mol %), PPI(PI**1**-*co*-DMAEM) (20:80 mol %), PI**1**/DMAEM (12:88 mol %).

The photo-DSC results of type I monomeric photoinitiator (PI**3**) together with commercial small molecular weight photoinitiator Irgacure 2959 are shown in Figure 4.18. It was observed that the initiator PI**3** exhibited higher reactivity than the monomeric and polymeric BP and AP derivative systems in HDDA. This was suggested to be caused by the different photoinitiation mechanisms between the photoinitiator systems. Unlike BP and AP derivatives, PI**3** does not require an electron donating agent such as tertiary amines to initiate the hydrogen abstraction mechanism. PI**3** and PPI**3** at a concentration of 1 mol% were found to show similar reactivity compared with Irgacure 2959 at 2 mol% concentration. The conversion values were also similar (70%) compared to Irgacure 2959.

The photopolymerization of PI**3** (chosen since it is the only one among the three PIs that is liquid at room temperature) by itself was also carried out using photo-DSC under the same conditions to investigate its reactivity as a monomer (Figure 4.19). It exhibited quite high reactivity with a conversion value around 60-65%. The low conversion value may be due to crosslinked polymer formation resulting from difunctional structure of this photoinitiator.

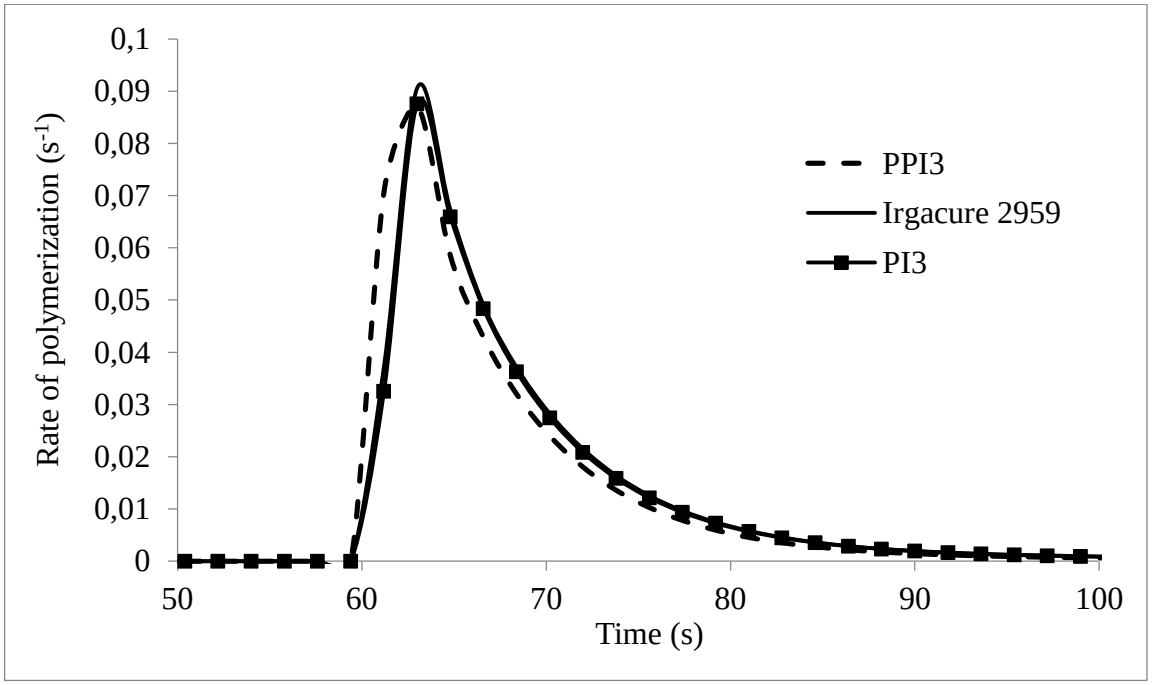

Figure 4.18. Rate-time and conversion-time plots for the photopolymerization of HDDA initiated by Irgacure 2959, PPI**3**, PI**3**. Photoinitiator concentration in monomer is 2 mol% for Irgacure 2959 and 1 mol% for PI**3** and PPI**3**.

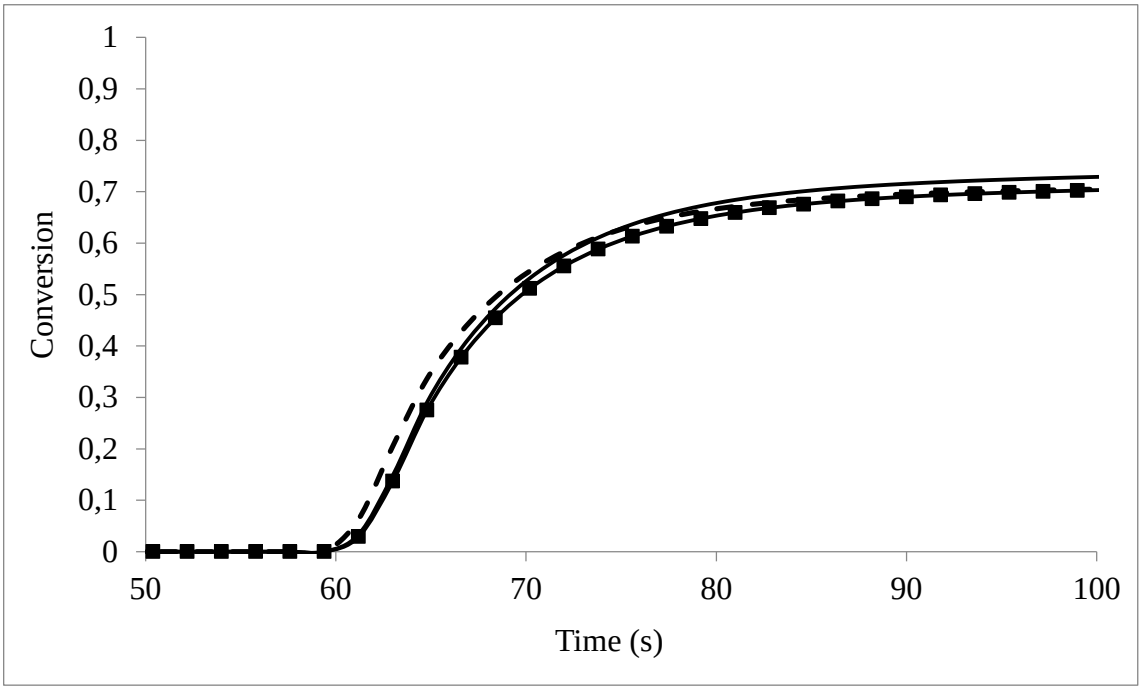

Figure 4.18. Rate-time and conversion-time plots for the photopolymerization of HDDA initiated by Irgacure 2959, PPI**3**, PI**3**. Photoinitiator concentration in monomer is 2 mol% for Irgacure 2959 and 1 mol% for PI**3** and PPI**3** (cont.).

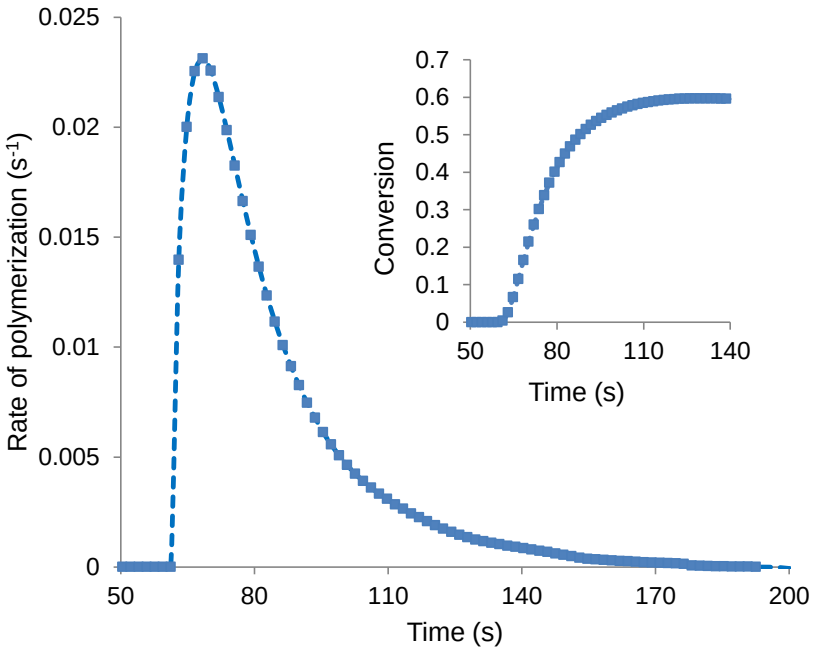

Figure 4.19. Rate-time and conversion-time plots for the photopolymerization of PI**3**.

We also performed photopolymerization of a monofunctional monomer (butyl methacrylate) using PI**3**, which gets incorporated into the polymer in addition to initiating the reaction. Solubility/swelling tests of the resulting copolymer showed that it is crosslinked. Hence we concluded that the difunctional nature of the PI**3** itself makes crosslinked copolymers possible even with monofunctional monomers (Figure 4.20).

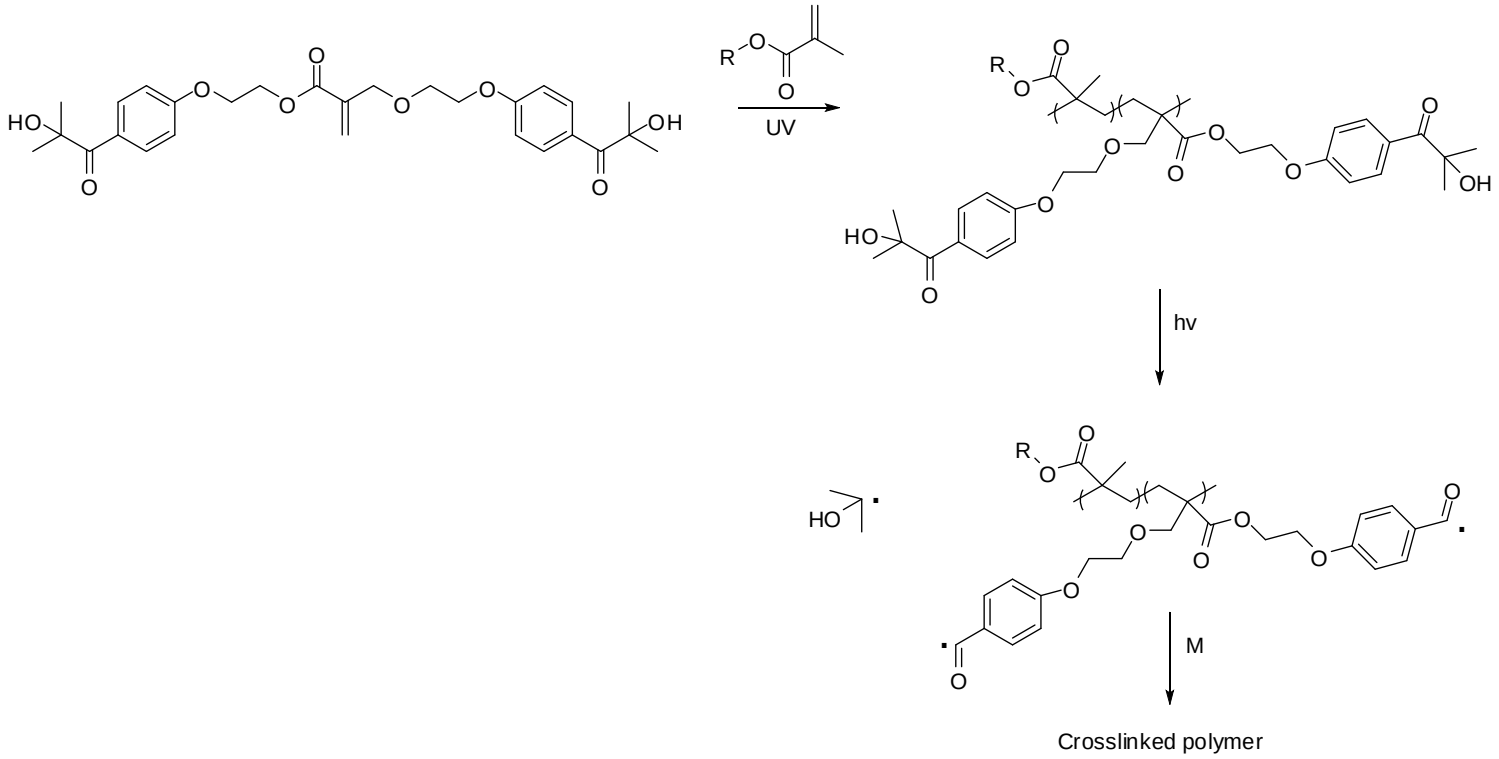

Figure 4.20. Photoinitiated free radical polymerization of butyl methacrylate by using PI**3**

5. CONCLUSION

Three novel monomeric (PI**1**, PI**2** and PI**3**) and four novel polymeric (PPI**1**, PPI**2**, PPI**3** and PPI(PI**1**-*co*-DMAEM)) photoinitiators based on AP, BP and Irgacure 2959 have been synthesized; PI**1**, PI**2** and PI**3** being the first difunctional methacrylate monomers (the two functional groups on a given monomer are identical). The photopolymerization of HDDA initiated by these photoinitiators and non-polymerizable commercial low molecular weight analogs was studied through photo-DSC. The BP-based photoinitiators (PI**1**, PPI**1** and PPI(PI**1**-*co*-DMAEM)) showed higher photoinitiating activity than BP itself, and also AP-based photoinitiators; polymeric ones being even more reactive than monomeric ones. PPI(**1**-*co*-DMAEM) has the extra advantages of elimination of an additional amine and non-toxicity. Synthesized PIs with better properties than commercial small molecule nonmonomeric analogues constitute a new class of PIs for potential use in UV curing applications. This PI can also be used as a crosslinker of monofunctional monomers during photopolymerization, probably a first. The design of difunctional PIs containing two different photoinitiating groups will be investigated in forthcoming work.

REFERENCES

1. Dietliker, K., T. Jung, J. Benkhoff, H. Kura, A. Matsumoto, H. Oka, D. Hristova, G. Gescheidt and G. Rist, "New Developments in Photoinitiators", *Macromolecular Symposia,* Vol. 217, pp. 77-97, 2004.

2. Cheng, L. and W. Shi, "Synthesis and Photoinitiating Behavior of Benzophenone-Based Polymeric Photoinitiators Used for UV Curing Coatings", *Progress in Organic Coatings*, Vol. 71, pp. 355-361, 2011.

3. Dietliker, K., R. Hüsler, J. L. Birbaum, S. Ilg, S. Villeneuve, K. Studer, T. Jung, J. Benkhoff, H. Kura, A. Matsumoto and H. Oka, "Advancements in Photoinitiators-Opening Up New Applications for Radiation Curing", *Progress in Organic Coatings,* Vol. 58, pp. 146-157, 2007.

4. Corrales, T., F. Catalina, C. Peinado and N.S. Allen, "Free Radical Macrophotoinitiators: An Overview on Recent Advances", *Journal of Photochemistry and Photobiology A: Chemistry*, Vol. 159, pp. 103-114, 2003.

5. Carlini, C., L. Angiolini, D. Caretti and E. Corelli, "Recent Advances on Photosensitive Polymers: Polymeric Photoinitiators", *Polymers for Advanced Technologies*, Vol. 7, pp. 379-384, 1996.

6. Yagci, Y., S. Jockush and N. J. Turro, "Photoinitiated Polymerization: Advances, Challenges, and Opportunities", *Macromolecules* , Vol. 43, pp. 6245-6260, 2010.

7. Wei, J., H. Wang, X. Jiang and J. Yin, "Study of Novel PU-Type Polymeric Photoinitiators Comprising of Side-Chain Benzophenone and Coinitiator Amine: Effect of Macromolecular Structure on Photopolymerization", *Macromolecular Chemistry and Physics,* Vol. 208, pp. 287-294, 2007.

8. Wei, J., R. Lu and F. Liu, "Novel, Highly Efficient Polymeric Benzophenone Photoinitiator Containing Coinitiator Moieties for Photopolymerization", *Polymers for Advanced Technol*ogies, Vol. 21, pp. 656-662, 2010.

9. Fouassier, J. P. and J. Lalevée, *Photoinitiators for Polymer Synthesis: Scope, Reactivity and Efficiency*, First Edition, Wiley-VCH Verlag GmbH & Co. KGaA, Weinheim, pp. 3-4, 2012.

10. Odian, G., *Principles of Polymerization*, Wiley-Interscience Press, New York, 1981.

11. Andrzejewska E., "Photopolymerization Kinetics of Multifunctional Monomers", *Progress in Polymer Science*, Vol. 26, pp. 605-665, 2001.

12. Dietliker, K., *In Chemistry and Technology of UV & EB Formulation for Coating Inks and Paints*: *Photoinitiators for Free Radical Cationic and Anionic Photopolymerization*, Second Edition, Vol. III, Ed. G. Bradley, SITA Technology Ltd, London, 1998.

13. Allonas, X., J. Lalevée, F. M. Savary and J. P. Fouassier, "Understanding the Reactivity of Photoinitiating Systems for Photopolymerization", *Polimery*, Vol. 51, pp. 491-498, 2006.

14. Arsu, N., I. Reetz, Y. Yagci and M. K. Mishra, *In Handbook of Vinyl Polymers: Radical Polymerization and Technology, Photoinitiated Radical Vinyl Polymerization*, Vol. 8, pp. 142-171, 2007.

15. Angiolini, L., D. Caretti, C. Carlini, E. Corelli and E. Salatelli, "Polymeric Photoinitiators Having Benzoin Methylether Moieties Connected to the Main Chain Through the Benzyl Aromatic Ring and Their Activity for Ultraviolet-Curable Coatings", *Polymer*, Vol. 40, pp. 7197-7207, 1999.

16. Groot, H. D. J., K. Dillingham, H. Deuring, H. J. Haitjema, F. J. V. Beijama, K. Hodd and S. Norrby, "Hydrophilic Polymeric Acylphospine Oxide Photoinitiators/ Crosslinkers for in Vivo Blue-Light Photopolymerization", *Biomacromolecules*, Vol. 2, pp. 1271-1278, 2001.

17. Allen, N. S., M. C. Marin, M. Edge, D. W. Davies, J. Garrett, F. Jones, S. Navaratnam and B. J. Parsons, "Photochemistry and Photoinduced Chemical Crosslinking Activity of Type I and II Co-reactive Photoinitiators in Acrylated Prepolymers", *Journal of Photochemistry and Photobiology A: Chemistry*, Vol. 126, pp. 135–149, 1999.

18. Wang, J., J. Cheng, J. Liu, Y. Gao and F. Sun, "Self-floating Ability and Initiating Gradient Photopolymerization of Acrylamide Aqueous Solution of a Water-soluble Polysiloxane Benzophenone Photoinitiator", *Green Chemistry*, Vol. 15, pp. 2457-2465, 2013.

19. Corrales, T., F. Catalina, C. Peinado, N. S. Allen, A. M. Rufs, C. Bueno and M. V. Encinas, "Photochemical Study and Photoinitiation Activity of Macroinitiators Based on Thioxanthone", *Polymer*, Vol. 43, pp. 4591-4597, 2002.

20. Wang, Y., X. Jiang and J. Yin, "Novel Polymeric Photoinitiators Comprising of Side-Chain Benzophenone and Coinitiator Amine: Photochemical and Photopolymerization Behaviors", *European Polymer Journal*, Vol. 45, pp. 437-447, 2009.

21. Wei, J., R. Lu and F. Liu, "Effect of Photosensitive Groups on the Photoefficiency of Polymeric Photoinitiators", *Journal of Polymer Research*, Vol. 18, pp. 1001-1008, 2011.

22. Wang, K., Y. Lu, P. Chen, J. Shi, H. Wang and Q. Yu, "Novel One-Component Polymeric Benzophenone Photoinitiator Containing Poly (ethylene glycol) as Hydrogen Donor", *Materials Chemistry and Physics*, Vol.143, pp.1391-1395, 2014.

23. Wei, J. and F. Liu, "Novel Highly Efficient Macrophotoinitiator Comprising Benzophenone, Coinitiator Amine, and Thio Moieties for Photopolymerization", *Macromolecules*, Vol. 42, pp. 5486-5491, 2009.

24. Wang, H., J. Wei, X. Jiang and J. Yin, "Highly Efficient Sulfur-Containing Polymeric Photoinitiators Bearing Side-Chain Benzophenone and Coinitiator Amine for Photopolymerization", *Journal of Photochemistry and Photobiology A: Chemistry,* Vol. 186, pp. 106-114, 2007.

25. Wang, H., J. Wei, X. Jiang and J. Yin, "Novel Chemical-Bonded Polymerizable Sulfur-Containing Photoinitiators Comprising the Structure of Planar *N*-phenylmaleimide and Benzophenone for Photopolymerization", *Polymer*, Vol. 47, pp. 4967-4975, 2006.

26. Karahan, O., D. Karaca Balta, N. Arsu and D. Avci, "Synthesis and Evaluations of Novel Photoinitiators with Side-Chain Benzophenone, Derived from Alkyl α-hyrdoxymethacrylates", *Journal of Photochemistry and Photobiology A: Chemistry* , Vol. 274, pp. 43-49, 2014.

27. Jiang, X. and J. Yin, "Polymeric Photoinitiator Containing In-Chain Thioxanthone and Coinitiator Amines", *Macromolecular Rapid Commun*ications, Vol. 25, pp. 748-752, 2004.

28. Wen, Y., X. Jiang, R. Liu and J. Yin, "Amphiphilic Polymeric Michler's Ketone (MK) Photoinitiators (APMKs) Containing PEO Chain and Coinitiator Amine", *Polymers Advanced Technol*ogies, Vol. 22, pp. 598-604, 2011.

29. Nayak, B. R. and L. J. Mathias, "A Novel Photoinimer for the Polymerization of Acrylates and Methacrylates", *Journal of Polymer Science: Part A: Polymer Chemistry*, Vol. 43, pp. 5661-5670, 2005.

30. Angiolini, L., D. Caretti, E. Corelli and C. Carlini, ''Copolymeric Systems with Pendant Thioxanthone and α-Morpholinoacetophenone Moieties as Photosensitizing

and Photoinitiating Agents for UV-Curable Pigmented Coatings", *Journal of Applied Polymer Science*, Vol. 55, pp. 1477-1488, 1995.

31. Angiolini, L., D. Caretti, E.Corelli, C. Carlini and P. A. Rolla, " Copolymeric Systems Bearing Side-Chain Thioxanthone and α-aminoacetophenone Moieties as Photoinitiators for Ultraviolet-Curable Pigmented Coatings", *Journal of Applied Polymer Science*, Vol. 64, pp. 2247-2258, 1997.

32. Angiolini, L., D. Caretti and E. Salatelli, "Synthesis and Photoinitiation Activity of Radical Polymeric Photoinitiators Bearing Side-Chain Camphorquinone Moieties", *Macromolecular Chemistry and Phys*ics, Vol. 201, pp. 2646-2653, 2000.

33. Allonas, X., J. P. Fouassier, L. Angiolini and D. Caretti, "Excited-State Properties of Camhorquinone Based Monomeric and Polymeric Photoinitiators", *Helvetica Chimica Acta.*, Vol. *84*, pp. 2577-2588, 2001.

34. Chen, Y., J. Loccufier, L. Vanmaele, E. Barriau and H. Frey, "Novel Multifunctional Polymeric Photoinitiators and Photo-Coinitiators Derived from Hyperbranched Polyglycerol", *Macromolecular Chemistry and Phys*ics, Vol. 208, pp. 1694-1706, 2007.

35. Xie, H., L. Hu, Y. Zhang and W. Shi, "Sulfur-Containing Hyperbranced Polymeric Photoinitiator End-Capped with Benzophenone and Tertiary Amine Moiteies Prepared via Simultaneous Double Thiol-Ene Click Reactions Used for UV Curing Coatings", *Progress in Organic Coatings,* Vol. 72, pp. 572-578, 2011.

36. Allen, N. S., T. Corrales, M. Edge, F. Catalina, M. Blanco-Pina and A. Green, ''Photochemistry and Photopolymerization Activities of Novel Alkylthiobenzophenone Photoinitiators", *European Polymer Journal,* Vol. 34, pp. 303-308, 1998.

37. Xie, H., L. Hu and W. Shi, "Synthesis and Photoinitiating Activity Study of Polymeric Photoinitiators Bearing BP Moiety Based on Hyperbranced Poly(ester-

amine) via Thiol-ene Click Reaction", *Journal of Applied Polymer Science*, Vol. 123, pp. 1494-1501, 2012.

38. Chen, Y., J. Loccufier, L. Vanmaele and H. Frey, "Novel Multifunctional Hyperbranched Polymeric Photoinitiators with Built-in Amine Coinitiators for UV-Curing", *Journal of Materials Chemistry*, Vol. 17, pp. 3389-3392, 2007.

39. Si, Q., X. Fan, Y. Liu, J. Kong, S. Wang and W. Qiao, "Synthesis and Characterization of Hyperbranched–Poly(siloxysilane)-Based Polymeric Photoinitiators", *Journal of Polymer Science Part A: Polymer Chemistry*, Vol. 44, pp. 3261-3270, 2006.

40. Wen, Y., X. Jiang, R. Liu and J. Yin, "Amphipathic Hyperbranched Polymeric Thioxanthone Photoinitiators (AHPTXs): Synthesis, Characterization and Photoinitiated Polymerization", *Polymer*, Vol. 50, pp. 3917-3923, 2009.

41. Lovell, L. G., J. W. Stansbury, D. C. Syrpes and C. N. Bowman, "Effects of Composition and Reactivity on the Reaction Kinetics of Dimethacrylate/ Dimethacrylate Copolymerizations", *Macromolecules*, Vol. 32, pp. 3913-3921, 1999.

42. Kilambi, H., E. R. Beckel, K. A. Berchtold, J. W. Stansbury and C. N. Bowman, "Influence of Molecular Dipole on Monoacrylate Monomer Reactivity", *Polymer*, Vol. 46, pp. 4735-4742, 2005.

43. Turro, N. J., *Modern Molecular Photochemistry*, University Science Books, Mill Valley, California, 1991.

44. Kim, S. K. and C. A. Guyman, "Effects of Polymerizable Organoclays on Oxygen Inhibition of Acrylate and Thiol-Acrylate Photopolymerizable", *Polymer*, Vol. 53, pp. 1640-1650, 2012.

45. Studer K., C. Decker, E. Beck and R. Schwalm, "Overcoming Oxygen Inhibition in UV-Curing of Acrylate Coatings by Carbon Dioxide Inerting, Part I", *Progress in Organic Coatings,* Vol. 48, pp. 92-100, 2003.

46. Lee, T. Y., C. A. Guymon, E. S. Jonsson and C. E. Hoyle, "The Effect of Monomer Structure on Oxygen Inhibition of (meth)acrylates Photopolymerization", *Polymer,* Vol. 45, pp. 6155-6162, 2004.

47. Ruiz, C. S. B., L. D. B. Machado, J. E. Volponi and E. S. Pino, "Oxygen Inhibition and Coating Thickness Effects on UV Radiation Curing of Weatherfast Clearcoats Studied by Photo-DSC", *Journal of Thermal Analysis and Calorimetry,* Vol. 75, pp. 507-512, 2004.

48. Anseth, K. S., C. N. Bowman and N. A. Peppas, "Polymerization Kinetics and Volume Relaxation Behavior of Photopolymerized Multifunctional Monomers Producing Highly Crosslinked Networks", *Journal of Polymer Science: Part A: Polymer Chemistry,* Vol. 32, pp. 139-1447, 1994.

49. Young, J. S., A. R. Kannurpatti and C. N. Bowman, "Effect of Comonomer Concentration and Functionality on Photopolymerization Rates, Mechanical Properties and Heterogeneity of the Polymer", *Macromolecular Chemistry and Physics*, Vol. 199, pp. 1043-1049, 1998.

50. Fouassier, J. P., *In Photoinitiation, Photopolymerization, and Photocuring: Fundamentals and Applications*, Hanser: Munich, 1995.

51. Davidson, S., *Exploring the Science, Technology and Application of UV and EB Curing*, Sita Technology Ltd, London, 1999.

52. Drobny, J. G., *Radiation Technology for Polymers,* CRC Press, Boca Raton, Florida, 2010.

53. Schwalm, R., *UV Coatings : Basics, Recent Developments and New Applications*, Elsevier, Oxford, 2007.

54. Rabek, J. F., *In Radiation Curing in Polymer Science and Technology*, J. P. Fouassier and J. F. Rabek, Eds.; Chapman & Hall, London, Vol. I, pp. 453-502, 1993.

55. Mathias, L. J. and S. H. Kusefoglu, "New Difunctional Methacrylate Ethers and Acetals: Readily Available Derivatives of Alpha-hydroxymethyl Acrylates", *Macromolecules*, Vol. 20, pp. 2039-2041, 1987.

56. Morizur, J. F., D. J. Irvine, J. J. Rawlins and L. J. Mathias, "Synthesis of New Acrylate-Based Nonionic Surfmers and Their Use in Heterophase Polymerization", *Macromolecules*, Vol.40, pp. 8938-8946, 2007.

57. Brandrup, J. and E. H. Immergut, *Polymer Handbook*, Wiley-Interscience, New York, 1975.